Journal of Field Robotics

WILEY

RESEARCH ARTICLE OPEN ACCESS

Enabling Under Ice Glider Operations: A Backseat Driver Approach

Yaomei Wang[1] | Benjamin Allsup[1] | Georgios Salavasidis[1] | Stephen Woodward[1] | Adeniyi Adenaya[1] | Mike Smart[1] | Alexis Johnson[1] | Felipe Marques Dos Santos[1] | Jake Ludgate[2] | Daniel Matterson[1] | Alvaro Lorenzo[1] | J. Alexander Brearley[3] | Alexander Brian Phillips[1]

[1]Marine Autonomous and Robotic Systems, National Oceanography Centre, Southampton, UK | [2]Ocean Technology and Engineering Group, National Oceanography Centre, Southampton, UK | [3]Brittish Antarctic Survey, Cambridge, UK

Correspondence: Yaomei Wang (yaomei.wang@noc.ac.uk)

Received: 4 December 2024 | **Revised:** 29 August 2025 | **Accepted:** 14 February 2026

Funding: Natural Environment Research Council, Grant/Award Number: NE/W004933/1; European Union's Horizon 2020, Grant/Award Number: 821001(SO_CHIC)

Keywords: autonomous under ice operations | backseat driver | Slocum gliders

ABSTRACT

Polar Oceans are key locations for forcing global ocean circulation, influencing both global climate and biogeochemical cycles. Due to restricted access to these seasonally and perennially ice-covered regions, these areas are severely undersampled. As such, there is an ongoing demand to expand the capabilities of marine robotics to enable observations here, especially during the winter months when many of the most important climate processes (e.g., dense water formation and carbon sequestration) occur. Underwater gliders are increasingly required to operate in ice-covered regions, both for short-term missions lasting days and long-term excursions extending over several months. The standard control system of Slocum gliders, while equipped with ice coping behaviors, is not designed for deliberate under-ice missions. To enhance the capabilities of Slocum gliders, the authors present a backseat driver system coupled with an upward-looking altimeter designed to enable more complex missions and ensure safe surfacing clear of the ice. The backseat driver is an additional control system that enables advanced decision-making using a combination of the glider's own state information and scientific sensor measurements. This backseat driver allows gliders to (1) change heading adaptively, (2) sense the presence of and avoid collisions with ice, (3) customize surfacing considering ice extent, and (4) trigger contingency behaviors in the event of faults beneath the ice. The developed backseat driver was tested through lab and field trials and has been deployed for a long-term deployment in the Weddell Sea as part of the UK's National Capability BIOPOLE program, with short-duration under-ice missions.

1 | Background and Related Work

Polar oceans such as the Southern Ocean are highly important for global ocean circulation and are critical regions for climate and biogeochemical cycling (Rintoul 2018). The lack of comprehensive and high-resolution data on oceanic processes in polar regions limits our understanding of ocean dynamics and their global implication for sea level rise, weather patterns, and climate change. As one of the least understood and most data-scarce regions on Earth, substantial effort has been invested in studying them. Polar research vessels allow the simultaneous deployment of multiple science instruments to gather information from polar regions; however, ice coverage restricts access to certain areas, limiting the extent and thoroughness of the research. Drilling a hole through the ice enables us to observe the ocean below, yet logistical challenges arise when accessing remote polar regions and conducting drilling operations in harsh environmental conditions. Moreover, drilling is often impractical on sea ice, particularly when it is thin or mobile. Since the measurements are typically point-based, spatial coverage is limited to the specific locations where holes are drilled, making it challenging to directly observe data between these points and complicating efforts to interpolate/extrapolate the information across larger areas. Since 2001, Argo floats have been deployed by Alfred Wegener Institute to the Southern Ocean with extended periods of intense ice conditions (Klatt et al. 2007). These floats are equipped with the ice-sensing algorithm and ice resistance hardware to improve their survival in ice-covered regions. The upgraded internal memory and under ice tracking ability, aided by Ranging and Fixing of Sound (RAFOS) sound sources, has enhanced the quality of the data collected. However, as Lagrangian platforms that rely on ocean currents for movement, the floats face challenges in maintaining horizontal control. This makes it difficult to direct them through specific regions of interest and to keep a consistent trajectory over extended periods, especially under the ice.

Unlike Argo floats, autonomous underwater vehicles (AUVs) are equipped with horizontal control systems that enhance navigation precision, improve maneuverability, and enable them to maintain a desired course. The operation of AUVs under ice began in 1972 when an unmanned Arctic research submersible was launched from Fletcher's Ice Island in the central Arctic, successfully completing a mission of over 17 miles in more than 4 h (Murphy 1972). In 1995, the International Submarine Engineering (ISE) Theseus AUV for laying fiber-optic cables in ice-covered waters was deployed near Ellesmere Island in the Arctic Ocean, achieving a cumulative distance of 13 km across all under-ice dives (Ferguson 1998). In January/February 2001, the AUV Autosub-2 was deployed from RRS James Clark Ross during a 27-day cruise (Brierley 2001). Equipped with a Simrad EK500 scientific echo sounder, Autosub-2 undertook 20 missions beneath sea ice and icebergs in the northern Weddell Sea, as well as in open water off the Antarctic Peninsula. The mission aimed to collect comparative data on the distribution and abundance of Antarctic krill in both open and ice-covered waters, measure sea ice thickness, assess the attenuation of photosynthetically active radiation by sea ice, and obtain underwater profiles of icebergs (Brierley et al. 2002). In total, Autosub completed over 275 km of transects beneath the sea ice. In 2010, an ISE Explorer AUV was deployed to the Canadian High Arctic for a bathymetric survey under ice. The vehicle operated under the ice for nearly 12 days, covering close to 1000 km before being recovered, aided by under-ice charging, long-range homing and short-range positioning techniques (Kaminski et al. 2010). In 2018, the Autosub Long Range (ALR), famously known as "Boaty Mcboatface", penetrated over 25 km under the Filchner and Ronne ice shelves in the Southern Weddell Sea (McPhail et al. 2019). In 2022, the ALR traveled over 40 km beneath the Dotson Ice Shelf, collecting data on currents, turbulence, water temperature, and salinity (Fanelli et al. 2025).

Unlike AUVs, which can maintain a constant depth and therefore keep their sensors at a fixed attitude for optimal orientation relative to the ice, standard underwater gliders performing "yo" maneuvers experience significant variations in pitch angle during ascent and descent. Operating gliders under ice is challenging. The standard operational procedure, which involves making multiple subsea dives and ascents (yo–yo pattern) before returning to the surface to acquire a Global Positioning System (GPS) fix for updating navigation and reconnecting with command-and-control systems, is clearly impractical in under-ice environments. Additionally, in an emergency, the ascent mode for underwater gliders, such as ejecting an abort weight to return to the surface for retrieval, is not feasible under ice.

Seagliders are capable of conducting under-ice missions by utilizing specialized ice-navigation features. In 2011, a Seaglider was successfully navigated under ice for 219 h, covering 155.6 km, aided by RAFOS acoustic sources in Davis Strait between Greenland and Baffin Island (Webster et al. 2014). However, access to the code controlling these ice-navigation features is currently restricted to the original developers, which limits the ability of third parties to further develop and optimize custom algorithms. In January 2019, a Slocum glider was deployed beneath the Nansen Ice Shelf and resurfaced 20 h later (Kerlin 2019). The mission was conducted through careful predeployment calculations and mission planning, but lacked adaptive control strategies to minimize risks associated with missions under ice.

As one of Europe's largest combined developers and operators of marine autonomous systems for oceanographic data gathering, the Marine Autonomous and Robotic Systems group at the National Oceanography Center in the UK operates a fleet of over 40 underwater robots consisting of a mixture of remotely operated vehicles, underwater gliders, and AUVs. The group's gliders are increasingly tasked with more complex missions, particularly in collecting ocean data beneath sea ice, both for short-term and long-term operations. Therefore, there is a need to enhance existing capabilities and develop new functionalities for the glider fleet. Efforts are now focused on equipping Slocum gliders with an adaptive control system, the backseat driver, to improve their ability to safely conduct under-ice missions and address dynamic conditions with reduced risk.

The backseat driver concept is not new for autonomous underwater systems. Motivated by the need for adaptive autonomy, code portability, and rapid reconfiguration of various AUVs, Eickstedt and Sideleau (2009) implemented a backseat driver architecture on a commercially available AUV, Iver2, manufactured by Ocean Server Technology. The backseat driver architecture was built based on the Mission Oriented Operating Suite-Interval Programming (MOOS-IvP), an autonomy software for supporting the operation of autonomous marine vehicles. An intelligent control component within the backseat driver generated command decisions for key vehicle states (such as speed, heading, and depth) and forwarded them to the main vehicle's dynamic control system. Conversely, the dynamic control component in the main vehicle control system executed these commands and fed back navigation state information to the backseat driver for continual decision refinement. To enable adaptive homing to a single beacon, a MOOS-IvP-based homing application was developed as a backseat driver and demonstrated on a Teledyne Gavia AUV (Keane et al. 2020). The application estimated the beacon's position and used this information to generate dynamic homing waypoints, thereby achieving adaptive maneuvering ability. Naglak et al. (2018) assembled a backseat controller, both hardware and

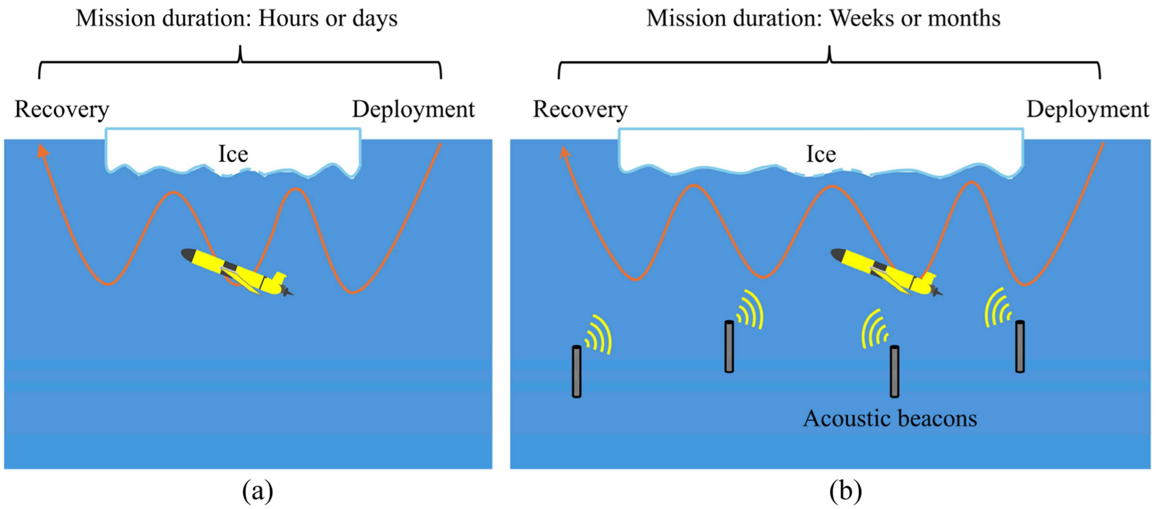

FIGURE 1 | Gliders' concept of under-ice operation: (a) short term and (b) long term. [Color figure can be viewed at wileyonlinelibrary.com]

software, on a General Dynamics Bluefin SandShark AUV. Unlike earlier systems, the backseat control system on the SandShark AUV was run on Robot Operating System (ROS), leveraging the rich pool of ROS contributors and open-source packages from different domains. The ROS-based backseat control system was also used on a Hydroid REMUS 100 AUV to facilitate sensor integration and autonomy test (Gallimore et al. 2018).

Similarly, the backseat driver concept has been applied to Slocum gliders. Wang et al. (2022) employed it across multiple gliders to delineate underwater oil patches; Engdahl et al. (2023) utilized the backseat driver to expand glider real-time data processing capabilities, broadening the real-time applications of sensor data.

However, its use to enhance Slocum gliders performance in under-ice missions, which are seeing increasing operational demand, remains unexplored. This paper serves to introduce a backseat driver system that enables Slocum gliders with the intelligence required for short-term under-ice missions. The contributions of this research are as follows:

1. *Backseat control system design:* Developed a backseat control system which can modify glider behavior, avoid ice collisions, and monitor risk in real-time for Slocum gliders conducting short-term missions adaptively in the challenging under-ice environment.
2. *Performance evaluation:* Evaluated the performance of backseat equipped Slocum glider comprehensively through lab tests and field trials.
3. *Weddell Sea demonstration:* Demonstrated the backseat equipped Slocum gliders in a deliberate under-ice mission in the Weddell Sea.

The remainder of this paper is organized as follows: Section 2 introduces the overall view of how gliders are operated in ice-covered regions, Section 3 describes the software and hardware implementations to enable Slocum gliders to operate safely under the ice, Section 4 presents the tests conducted in both lab and open ocean (ice free), whereas Section 5 shows the results of utilizing the adaptive control system during glider deployments under the ice. Section 6 presents conclusions and discusses future improvements.

2 | Concept of Operations

According to the extent of ice, the polar oceans can be divided into the following zones (Cochlan 2008; Montie et al. 2020): (1) permanently open ocean zone, (2) marginal and seasonal ice zone, (3) perennial ice zone, and (4) coastal and continental shelf zone. The operation of gliders under ice faces various challenges, primarily related to the ice extent in different zones and the scientific requirement of mission length. As such, operations are typically classified as short-term under-ice operation (hours or days, as shown in Figure 1a) and long-term under-ice operation (weeks or months, as shown in Figure 1b).

2.1 | Short-Term Under-Ice Operation

Short-term operation of underwater gliders beneath the ice can be crucial for a variety of reasons. It offers an opportunity to test and calibrate sensors and instruments in polar conditions before committing to long-term deployments. In addition, short-term under-ice deployments can be used to conduct preliminary assessments of environmental conditions or ice cover, which can inform the planning of more extensive long-term under-ice missions. It is particularly useful for understanding rapid processes when high temporal resolution data is required to capture detailed changes over shorter timescales. Researchers can adjust mission parameters or deployment locations in response to emerging phenomena or urgent research needs.

A glider in a short-term under-ice operation needs to surface to communicate or get GPS fixes every few hours or days. This can happen in the marginal ice zone, where the glider can access the surface opportunistically, or in a continuous ice region, where a mission only involves a short-term penetration into the ice-covered area and a subsequent exit. The glider is typically equipped with ice-sensing algorithms for safe climbing and surfacing. Additional underwater navigation devices may be

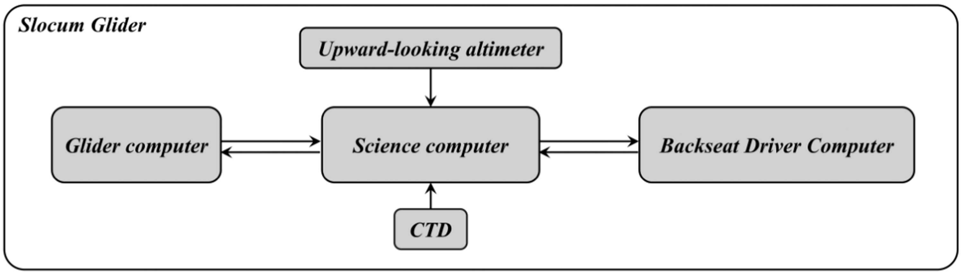

FIGURE 2 | Proposed high-level architecture including a backseat driver control system and an upward-looking altimeter. CTD, conductivity–temperature–depth.

unnecessary since the positioning error most likely is within acceptable limits, considering the length of the mission.

2.2 | Long-Term Under-Ice Operation

As the polar regions experience significant seasonal and annual changes in ice cover, temperature, and biological activity, continuous data collection across different seasons and years can provide insights into these variations and their impacts.

Long-term operation of a glider under ice involves piloting in the areas where ice remains for several months or even years, such as in the perennial ice zone or during the winter season in the seasonal ice zone. The glider estimates its underwater position using dead reckoning (Woithe et al. 2011) and only receives GPS fixes at the end of a mission. As such, accurate underwater navigation typically requires the support from external aiding infrastructure, such as acoustic positioning systems (Wang et al. 2025), to ensure reliable path following. Additionally, ice-sensing algorithms are required to prevent collisions with ice both during the mission and when surfacing at the end.

Since short-term under-ice operations can inform long-term strategies, this preliminary research focuses on the development of gliders designed for short-term operations beneath the ice.

3 | Technical Description

3.1 | Overview

In the standard control system of Teledyne Webb Research (TWR) Slocum gliders (Jones et al. 2014), which is equipped with ice coping behavior, a glider is considered "trapped under ice" if it cannot establish communication or receive GPS signals when it surfaces or maintains the same depth while attempting to surface or climb. In this case, recovery mode is activated and the glider sequences through different recovery missions depending on the flight performance and the number of times the missions have been run. However, this is not designed for deliberate under-ice missions and can stop a glider from entering an ice-covered area. To advance the capabilities of standard Slocum gliders under ice, a high-level architecture is designed by the authors, which incorporates a backseat driver on the Slocum gliders. The frontseat (in other words, the standard control system) and backseat paradigm is a collaborative approach to system design. It is frequently applied in intricate systems that require a tiered control structure to handle tasks involving high-stakes decision-making and adaptability. The frontseat is the main system responsible for low-level operations, such as adjusting buoyancy, steering, and executing specific navigational commands to stay on course. It operates as the primary layer in the glider's control system, ensuring that the glider can execute specific, predefined actions with minimal delay. The backseat, on the other hand, is a high-level system tasked with strategic planning, monitoring, and guidance. It focuses on broad objectives, mission parameters, and making adaptive decisions based on real-time feedback. Since it is less time-sensitive, the backseat can undertake more complex computations and strategic analysis, making high-level decisions that influence the frontseat's action.

The Slocum glider backseat driver in this work is designed to enhance the operation of the frontseat, which provides advanced control and management features, allowing operators to better manage the glider's missions and data collection tasks (Wang et al. 2021). The glider runs a modified version of the Slocum firmware that allows the external controller (backseat) integration. The frontseat runs standard missions, and the backseat driver computer is able to monitor information provided by the frontseat and to modify the missions in real-time. More specifically, the work proposes a backseat driver control system coupled with an upward-looking altimeter designed to enable a more complex under-ice mission design and ensure ice clear safe surfacing (Figure 2). The backseat driver control system monitors the state of the glider and the sensor measurements to manage the execution of an under-ice mission through the connection to the glider science computer; while the upward-looking altimeter integrated to the science computer helps detect the existence of ice. The integration of the upward-looking altimeter and implementation of the backseat driver necessitate modifications to the standard TWR Slocum glider. These enhancements allow gliders to detect ice with ice-sensing strategies and monitor hardware faults through different sensors inputs (conductivity–temperature–depth [CTD] measurements, upward-looking altitude, onboard power, etc.). Consequently, the gliders can autonomously process this information and make advanced decisions without requiring direct user inputs.

3.2 | Backseat Driver Control System

The backseat driver control system illustrated in this paper for conducting short-term under ice missions comprises a backseat driver interface, a mission controller module, and a hardware fault monitor module (see Figure 3). They allow a glider to (1) change its heading adaptively, (2) sense the presence of and

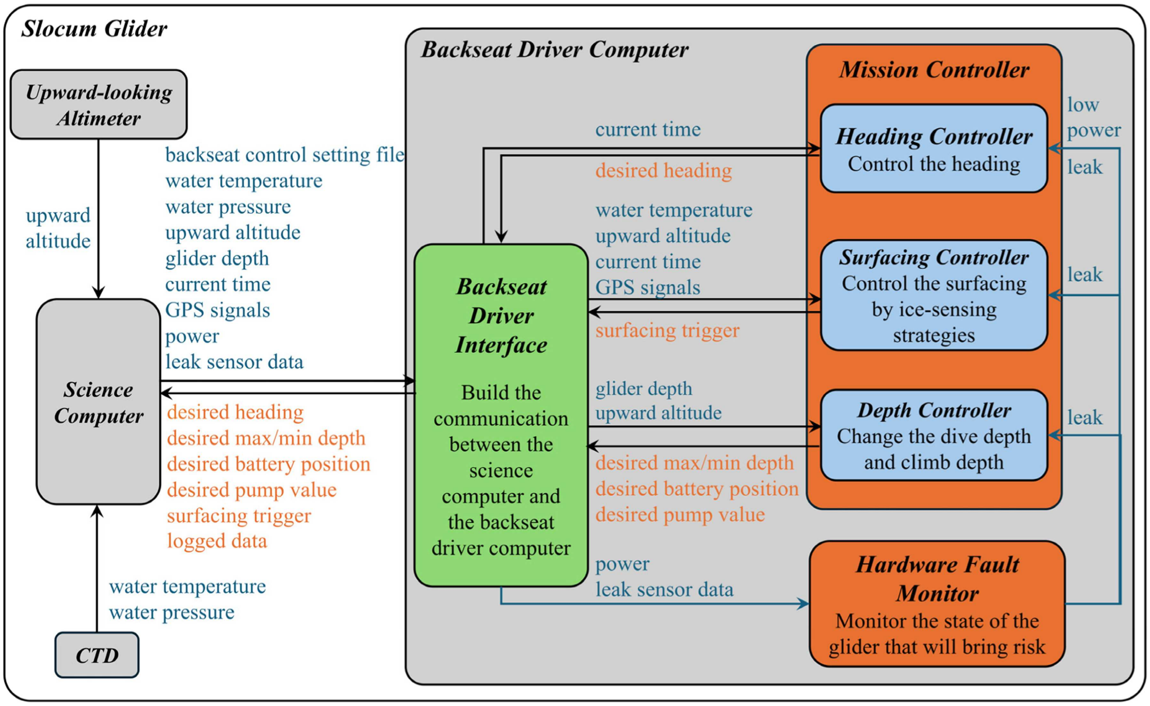

FIGURE 3 | The control architecture of the backseat driver for Slocum gliders conducting short-term under-ice missions. CTD, conductivity–temperature–depth; GPS, Global Positioning System. [Color figure can be viewed at wileyonlinelibrary.com]

avoid collisions with ice, (3) surface at a customized time considering ice extent, and (4) replan its missions in the event of hardware faults whilst operating beneath the surface ice.

3.2.1 | Backseat Driver Interface

The backseat driver interface is a generic module that is standard for any backseat driver implementation. This component oversees communications with the frontseat through a serial line. The backseat driver interface allows components in the backseat driver to monitor changes in the glider's state (e.g., depth, heading, and power available) and science sensor measurements (e.g., temperature and salinity) and then acts as an interface to allow the backseat driver components to trigger changes to the glider state. The interface also allows data in the backseat driver to be logged in the log folder in the science computer with a customized name, which facilitates the monitoring of the backseat driver's performance in controlling gliders. The interface component implements a standard communication protocol that also enables communication between the remote pilots and the backseat driver, taking advantage of the ability to read and write files from and to the Slocum navigation computer. A backseat control setting file, which customizes the control of the backseat driver, can then be sent to the backseat driver computer.

3.2.2 | Mission Controller

For a short-term under-ice mission controlled by the backseat driver, a glider is deployed to operate beneath the ice for a period ranging from several hours to a few days. During this time, the glider is directed to change its heading to eventually find the way to exit the ice-covered area. If there is no hardware fault detected, the glider does not need to surface to either obtain a GPS fix or transmit data during the mission, as the mission duration is short and the positioning error remains within acceptable limits. At the top of each ascent whilst under ice, the glider must use its onboard sensors to determine the ice depth and to turn to dive again before colliding with the ice and the associated risk of entrapment or damage (and similarly as the glider approaches the sea floor). Upon completing an under-ice mission, the glider typically traverses the marginal ice zone, which includes broken and melting ice, a mix of fresh and salt water, and open ocean. Therefore, the glider is programmed to activate a surfacing behavior only if no ice is detected at the surface. In the event of a threat to system integrity, the backseat driver is responsible for initiating contingency behaviors to ensure the glider's safety and mission success.

1. Heading controller

   When a glider is under the control of the backseat driver, the heading controller can command a change in the glider's heading at a specific time. This capability is particularly useful in under-ice scenarios where the glider may need to adjust its course due to unexpected ice conditions. The heading of the glider is adjusted in the following scenarios by the backseat driver system developed in this work:
   - The glider is required to go into the ice-covered area with a constant heading for a certain amount of time and then come out of the ice-covered area with another constant heading.
   - When there is a leak detected within the glider, the glider is commanded to come out of the ice-covered area with a constant heading.
   - When the power available onboard the glider is lower than a threshold value, the glider is commanded to come out of the ice-covered area with a constant heading.

The commanded headings in these scenarios are defined in the backseat control setting file and are sent by the backseat driver to the frontseat to update the desired heading value in the "set heading" behavior of the glider.

2. Depth controller

A standard Slocum glider utilizes a depth control system to navigate in the underwater environment efficiently and safely. This depth controller is responsible for critical functions: (1) to adjust glider's buoyancy to control ascent and descent through the water column, ensure that the glider remains within the desired depth ranges and gathers accurate and relevant mission data; (2) to prevent collisions with the sea bottom by continuously monitoring the glider's distance relative to the seabed with the use of a downward-looking altimeter.

Another depth controller is included in the backseat driver system for under ice control, supplementing the existing depth controller on the standard glider. One objective of incorporating the additional depth controller is to enhance safe navigation by maintaining the glider at an optimal minimum depth and a secure upward-looking altitude, thereby effectively preventing collision with the ice above. In this scenario, a reactive ice avoidance strategy should be responsible for computing and updating a safe minimum depth demand. This reactive ice avoidance strategy takes measurements from the upward-looking altimeter and the glider's depth sensor, and the glider is commanded to dive either when its depth is lower than the desired minimum depth or the upward-looking altitude is lower than a safe distance value. Another objective of incorporating the depth controller is to mitigate the risk of leaks. In the event of a leak, the depth controller commands the glider to ascend to a shallower depth and operate in a shallow depth range, thereby reducing the hydrostatic pressure on the glider. Furthermore, the backseat depth controller instructs the glider to rise to the water surface to assess the availability of GPS signals prior to activating surfacing behavior. The backseat driver initiates depth control only after the glider completes its initial shallow dive, ensuring an immediate surfacing in case of any issues with the backseat driver interface or the backseat control file.

3. Surfacing controller

A glider is expected to surface to transmit data or to be recovered at the end of a mission. Because of the presence of surface ice and requirements of mission duration, the surfacing behavior is activated by a combination of control factors, including ice-sensing strategies and permitted surfacing time. There are physical, biological, chemical, and acoustic indicators of ice; however, the glider can only use a limited suite of low-power sensors to determine ice presence, thereby regulating its surfacing and depth adjustments. In this work, only an upward-looking altimeter is added to a standard Slocum glider and the presence of ice is sensed by: (1) median temperature of the upper water column, (2) ice draft, (3) ice edge, and (4) GPS signals received by the glider.

3.2.2.1 | Median Temperature of the Upper Water Column

The concept of employing the median temperature of the upper water column to regulate the surfacing of a glider in icy regions is derived from the ice detection algorithm utilized in polar floats (Klatt et al. 2007; Riser et al. 2018). The ocean's mixed layer is the upper portion of the water column where properties like temperature, salinity, and density remain relatively consistent due to the mixing effects of wind, waves, and currents. In the Weddell Sea, the temperature in the mixed layer is close to the freezing point if there is ice on the water surface. During its profile ascent, the ice-sensing algorithm used in a float measures the temperature of the water column and calculates the median temperature of the upper water column, which lies within the mixed layer. The median temperature is used instead of the mean temperature to reduce the influence of outliers or sudden temperature spikes. Should the median temperature fall below a defined threshold temperature, it is anticipated that the water surface is enveloped by ice, and the float delays surfacing to protect itself from potential damage and dive again. Conversely, if the median temperature surpasses the threshold, it is anticipated that the water surface is devoid of ice, allowing the float to surface. Relying on the median temperature to govern the surfacing of floats proves reliable in winter, given the consistent temperature of the upper water column throughout its height (Sugimoto 2022). Nonetheless, during the summer, the temperature within the presumed upper water column varies, owing to fluctuations in the depth of the actual mixed layer (Sallée et al. 2021). Consequently, in summertime, floats do not rely on the median temperature of a single profile for surfacing control but rather consider the median temperature across multiple consecutive profiles. If, through comparing the median temperature of the upper water column with the threshold temperature across these profiles, it is anticipated that the water surface is ice-free, floats can be instructed to surface.

For the application of using median temperature to detect ice in the Slocum glider, the setting of the upper water column, such as the depth range of the upper water column, the threshold temperature, and the number of consecutive yos for checking the median temperature, is defined in the backseat setting file and should be sent to the backseat driver before an under-ice mission.

3.2.2.2 | Ice Draft

Ice draft is the vertical distance from the bottom of the ice to the water surface. It represents how much the ice is submerged below the waterline, as opposed to the ice freeboard, which is the portion above the waterline (Coppolaro 2018). Ice draft can be measured by the disparity between the water depth of the glider and its upward altitude (see Figure 4). When a glider is operating under ice, the CTD sensor measures the water depth, while the upward-looking altimeter determines the altitude to the ice above. The ice draft D_i is computed as

$$D_\mathrm{i} = D_\mathrm{p} - \frac{S_\mathrm{real}}{S_\mathrm{raw}} * D_\mathrm{a}^\mathrm{r} * \cos(\theta) - \Delta x * \sin(\theta) \in \begin{cases} (-\infty, b), & \text{uncertainty}, \\ (b, +\infty), & \text{ice}, \end{cases} \tag{1}$$

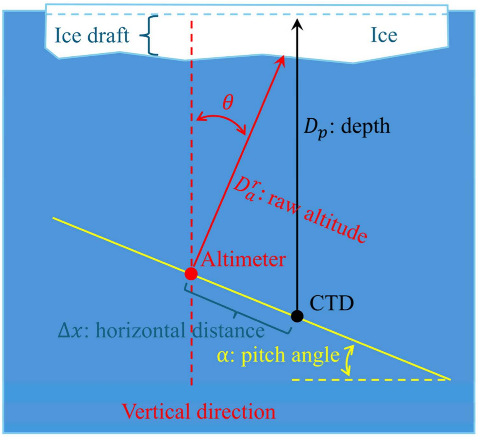

FIGURE 4 | Ice draft derived from the depth detected by the CTD sensor and the altitude detected by the upward-looking altimeter. CTD, conductivity–temperature–depth. [Color figure can be viewed at wileyonlinelibrary.com]

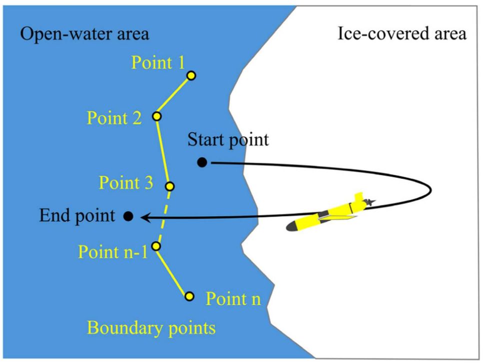

FIGURE 5 | A boundary generated by the ice edge, which is used to instruct the surfacing behavior of a glider. [Color figure can be viewed at wileyonlinelibrary.com]

where D_p is the depth measured by the CTD sensor, S_{real} is real sound speed at the point of altimeter, S_{raw} is the sound speed used in the altimeter, D_a^r is the raw distance measured by the upward-looking altimeter, θ is the measurement angle of the altimeter with respect to the vertical direction, Δx is the horizontal distance between the altimeter and the CTD sensor when the glider is level, and b is the minimum detectable submerged ice thickness which is a positive value. When the glider is level (pitch angle $\alpha = 0°$), the altimeter's measurement angle θ equals its physical mounting angle of 27°. As the glider climbs ($\alpha > 0$) or dives ($\alpha < 0$), the measurement angle is adjusted according to $\theta = 27° - \alpha$. Throughout a mission, the glider's pitch angle is continuously monitored in real-time. However, motion-induced fluctuations affect the accuracy of the measurements. To mitigate this issue, a median filter is introduced to smooth the raw data, providing a reliable pitch angle that is subsequently used to determine the altimeter's measurement angle.

Ideally, the surface is detected to be free of ice only if the measured ice draft is 0 m. However, owing to uncertainties stemming from the sensor measurements (such as upward-looking altitude, CTD depth, and glider pitch angle) and the influence from the environment, it is hard to measure the ice draft close to 0 m. The measured ice draft value can only reflect the submerged ice thickness when it falls within the range of $(b, +\infty)$.

3.2.2.3 | Ice Edge

Ice edge refers to the boundary between open-water area and ice-covered area and can be monitored by various methods, such as satellite remote-sensing and numerical models. Satellite imagery is a critical tool for monitoring ice. Satellite images can be generated by passive microwave sensors, optical sensors, and synthetic aperture radar. Instruments like the Special Sensor Microwave/Imager (SSM/I) and the Advanced Microwave Scanning Radiometer-Earth Observing System (AMSR-E) are passive microwave sensors. These sensors measure microwave radiation emitted by the Earth's surface, which varies between open water and ice. Sensors like Moderate Resolution Imaging Spectroradiometer (MODIS) provide high-resolution optical images that can be used to observe ice when conditions are clear (i.e., no cloud). Instruments like those on the Sentinel-1 satellites provide high-resolution radar images that can penetrate clouds and darkness, offering detailed information about ice. Satellite images are divided into grid cells, each grid cell may contain a percentage value representing ice concentration, which indicates the fraction of the cell covered by ice. The size of the grid cells depends on the sensor's resolution. For example, AMSR-E has a resolution of about 25 km, while MODIS can provide data at 1 km resolution. Numerical models simulate ice dynamics by integrating satellite data, in situ measurements, and oceanographic models. These models help predict future changes in the ice edge. IceNet is a deep learning model developed by the British Antarctic Survey for predicting sea ice concentration, which can provide a spatial resolution of 25 km (Andersson et al. 2021). It utilizes artificial intelligence to improve the accuracy and efficiency of sea ice forecasts, which are critical for understanding climate change and supporting navigation and operations in polar regions. Community Ice CodE is a widely used sea ice model developed by the Los Alamos National Laboratory. It includes detailed representations of sea ice thermodynamics, dynamics, and ice thickness distribution (Chassignet et al. 2020).

A boundary can be established by utilizing the predicted ice edge determined by glider pilots based on satellite images and/or numerical models, which delineates the transition from ice-covered areas to open-water areas, informed by the anticipated time required for a glider to complete its under-ice mission (Figure 5). The backseat driver notifies the glider when it is in the open-water area defined by the boundary. It should be noted that the ice edge is dynamic, and the glider's location can be unreliable without any external navigation support, such as GPS fixes or underwater acoustic-aided positioning systems, over extended periods.

3.2.2.4 | GPS

The existence of ice prohibits gliders from reaching the surface to obtain GPS signals. Thus, the GPS connectivity serves as an indicator of ice conditions on the water surface. The glider can be controlled by the backseat driver to reposition its pitch battery forward and to be slightly positively buoyant when it is close to the surface (Figure 6). In this scenario, the glider tilts

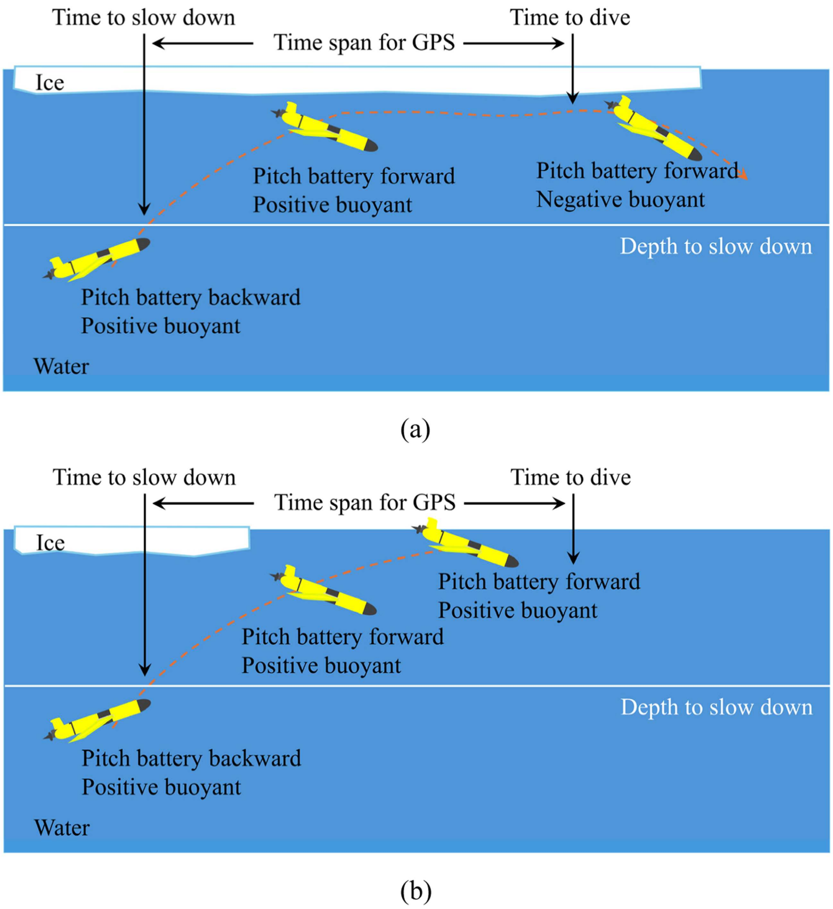

FIGURE 6 | The control of a glider to reach the surface to get GPS signals in an under-ice mission: (a) the surface is covered by ice and (b) the surface is free of ice. GPS, Global Positioning System. [Color figure can be viewed at wileyonlinelibrary.com]

downward, enabling the GPS sensor located at the tail to reach the surface first, without inflating the air bladder. These actions result in the glider making gentle climbing, reducing the chances of the glider becoming stuck if the surface is still ice-covered. The backseat driver also monitors the GPS signals to confirm a signal has been acquired. If the GPS status indicates a lack of GPS signals reception within a permitted time duration, the glider is commanded by the backseat driver to submerge (Figure 6a); otherwise, it is instructed to surface (Figure 6b).

The backseat driver checks the median temperature, ice draft, ice edge and surfacing time when the glider is climbing before checking GPS signals and controlling the surfacing behavior (Figure 7). Ideally, the glider surfaces only when all four ice-sensing strategies confirm the absence of ice on the surface and the designated surfacing time has been reached. However, due to uncertainties inherent in the ice-sensing methodologies, certain strategies may erroneously indicate ice presence for prolonged periods. To mitigate this, a surfacing control framework with multiple urgency levels (Figure 8) has been implemented, where each level utilizes a distinct combination of ice-sensing strategies alongside surfacing time parameters to minimize false ice detection. This framework consists of five independent urgency levels, each requiring one or more ice-sensing strategies to verify ice absence on the water surface and confirming surfacing time before initiating a climb for GPS signal acquisition, with the exception of the highest urgency level, which is dedicated to monitoring leak signals. In the urgency level where fewer ice-sensing strategies are employed, ice detection becomes more stringent. For example, at the median high urgency level, there are two sub-levels, each capable of independently triggering the glider's ascent to acquire GPS signals. The ice edge 1 will be more conservative and stricter than the ice edge 2 used in the low urgency level to confirm the absence of ice on the water surface. The principle also applies to surfacing time.

3.2.3 | *Hardware Fault Monitor*

As a complex mechanical device encompassing a power system, navigation system, buoyancy system, sensor system, control system, and so forth, Slocum gliders are susceptible to a range of potential hardware faults. The backseat driver is designed to monitor two critical hardware states in real-time that significantly impact mission completion and glider retrieval: the remaining battery power and voltages of leak detection sensors. Should any faults arise related to onboard power or hull sealing, the backseat driver generates contingency behaviors to mitigate the risk of losing the glider beneath the ice forever.

1. Remaining battery power

   The backseat driver checks the remaining battery power on a glider during the whole mission duration, evaluating either the battery voltage or coulomb measurements. If the glider is in the process of entering an ice area and the lower power state is detected, the glider is commanded by the backseat driver to exit the ice area by changing its desired heading immediately. At the same time, the

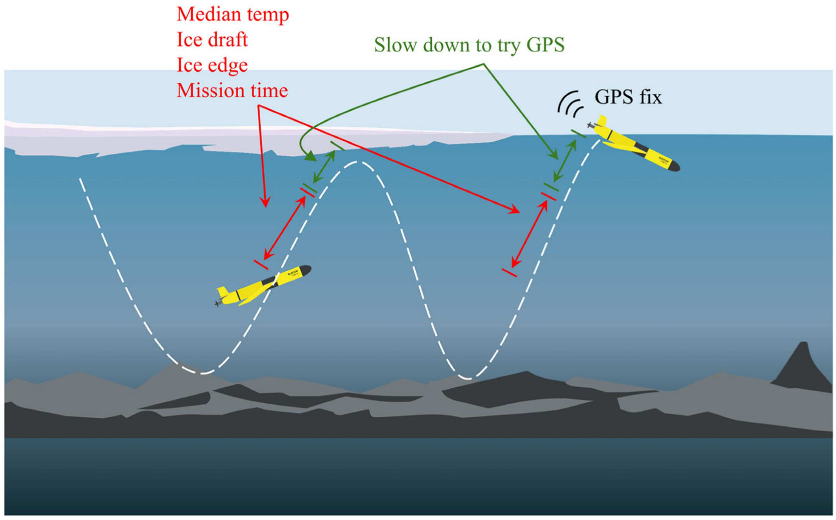

FIGURE 7 | The surfacing control used by the backseat driver, which checks the ice-sensing strategies and mission time when the glider is climbing before slowing down to check GPS signals. GPS, Global Positioning System. [Color figure can be viewed at wileyonlinelibrary.com]

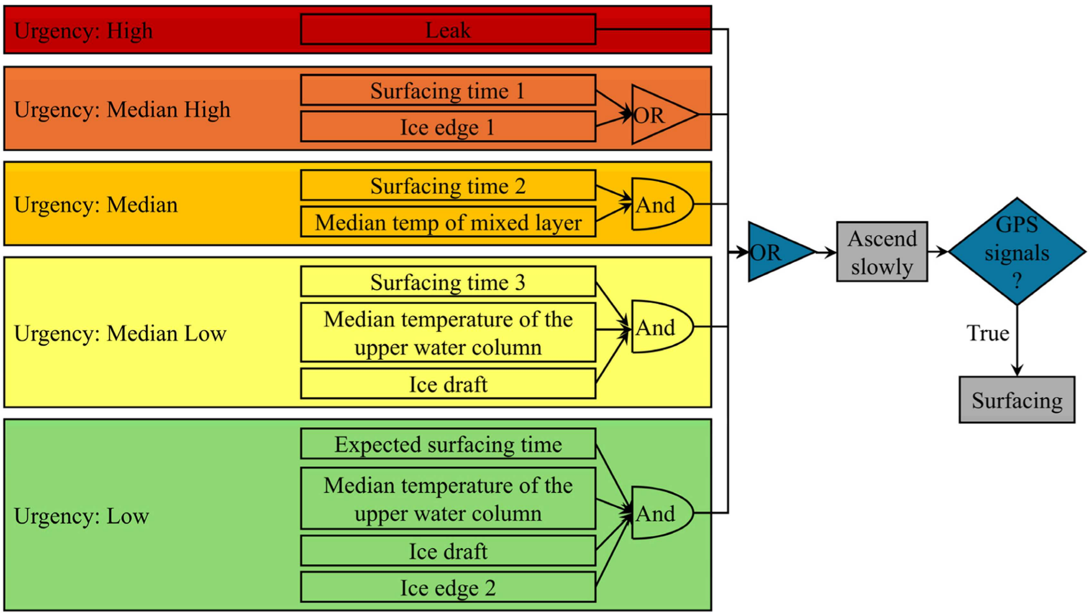

FIGURE 8 | Urgency levels and their control factors, which trigger a climbing to the surface to check GPS signals. GPS, Global Positioning System. [Color figure can be viewed at wileyonlinelibrary.com]

surfacing time is updated, which expects the glider to surface at the same surfacing location as the original surfacing plan (Figure 9a):

$$\text{Updated surfacing time} = 2 * T_e + T_l - 2 * T_p, \qquad (2)$$

in which T_e is the original expected surfacing time, T_l is the time when the low-power state is detected, and T_p is the planned heading change time. Otherwise, if the lower power state is detected when the glider is exiting the ice area, the original surfacing time is used (Figure 9b).

2. Leak

The Slocum glider is equipped with a leak detection system, which consists of two leak sensors placed on the bottom of the front and aft caps to ensure the integrity and safety of its operations. The sensors detect the presence of water within the normally dry interior spaces of the glider and are crucial for early detection of water ingress, which can prevent damage to the electronics and other sensitive components. These sensors typically output 2.5 V under normal conditions. When exposed to moisture, the circuit is shorted, and any reading below a default threshold of 2 V triggers an abort due to leak detection in a standard Slocum glider.

However, an abort should be prohibited when the glider is under ice. The backseat driver handles the fault from the leak by checking the voltage measurement from the leak sensors and comparing it with a threshold value. If the voltage measured by the forward leak detect sensor or the

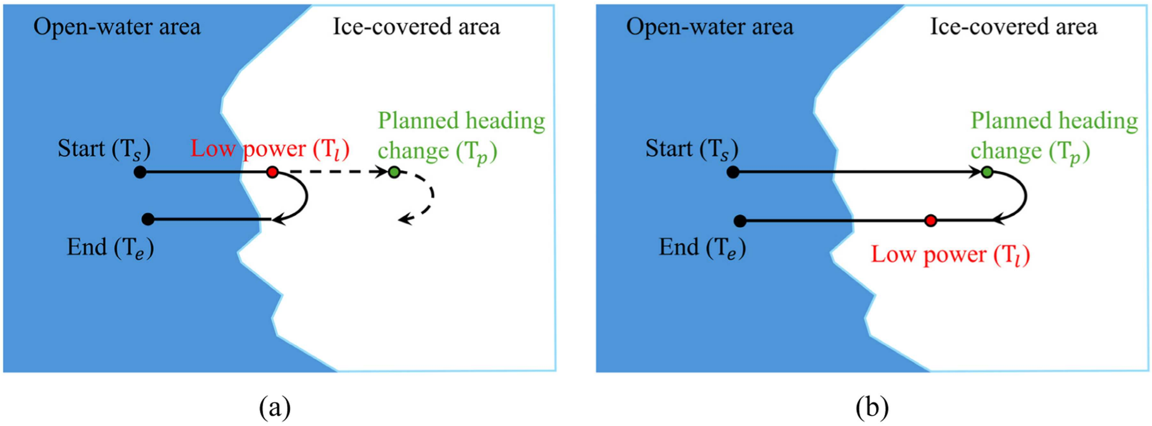

FIGURE 9 | Lower power state is detected in two situations: (a) when the glider is entering an ice area and (b) when the glider is exiting an ice area. [Color figure can be viewed at wileyonlinelibrary.com]

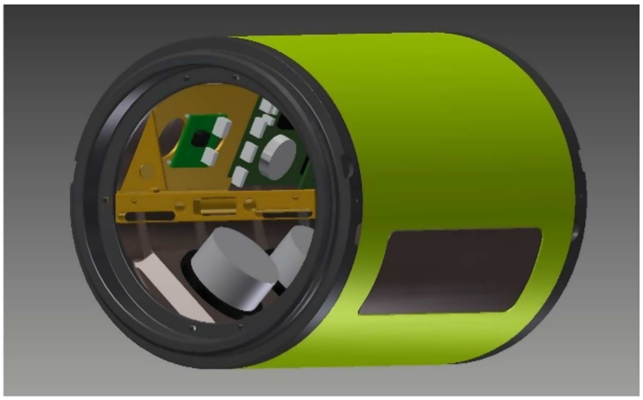

FIGURE 10 | Backseat driver processor being integrated inside the Slocum glider science bay. [Color figure can be viewed at wileyonlinelibrary.com]

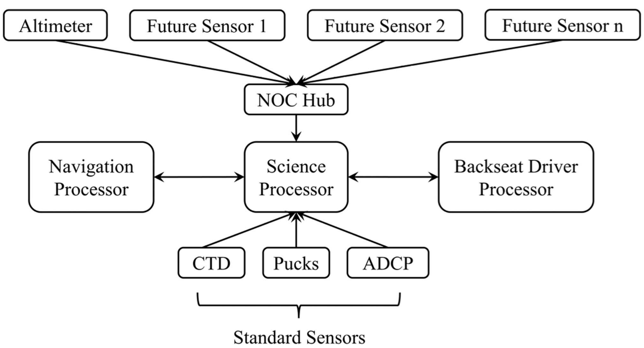

FIGURE 11 | Backseat driver microprocessor and National Oceanography Centre (NOC) hub prototype glider integration. ADCP, Acoustic Doppler Current Profiler; CTD, conductivity–temperature–depth.

aft leak detect sensor is lower than the threshold value, the glider is commanded to conduct configurable contingency behaviors: (1) go to a shallower depth range for its yo behavior to decrease the water pressure on the glider, and (2) change its heading to exit the ice-covered area. The glider is also commanded to climb to the water surface for GPS acquisition every several yos. If no GPS signal is detected, the backseat driver commands the glider to dive; otherwise, it commands the glider to activate a surfacing behavior.

3.3 | Hardware Integration

The backseat driver processor is accommodated inside the Slocum glider's science bay (Figure 10) to get direct access to the science computer, which is the way that the backseat driver processor can interact with the frontseat and oversee all glider sensors (Figure 11). With these sensor measurements, algorithms running on the backseat driver processor can then retask some elements of the glider navigation computer. A National Oceanography Centre (NOC) hub serves as an interface system that allows the altimeter and a range of future glider sensors (acoustic signal receivers, wet chemical sensors, etc.) to connect to the glider architecture and allow the backseat driver to act on their data. Initially, the backseat driver algorithms were implemented on a Raspberry Pi microprocessor. This was replaced with a bespoke microprocessor using a similar architecture but operating at significantly reduced power consumption.

Slocum G2 and G3 gliders are fitted with an Airmar (170/200 kHz) altimeter, with a 0–100-m range transducer. It is mounted on the front of the ballast pump assembly, and its electronics are supported on the cylinder of the ballast pump assembly. The transducer leads feed through a bulkhead connector on the front-end cap. The transducer is oriented so that it is parallel to a flat sea bottom at a nominal dive angle of 26°. This sensor only provides distance as an output. In this orientation, it would be unable to make any measurements of the upward altitude (distance below the ice) or provide useful information to infer ice draft.

The altimeter Impact Subsea ISA500 (Impact Subsea 2024), with a 0.1–120-m range, is selected as the upward-looking altimeter to detect ice on the surface based on its low-power consumption and its characteristics, which meet the requirements of field missions. In addition to the slightly longer range, the ISA500 is able to provide multiecho output, potentially providing more information about the water column. A right-angle housing configuration is chosen, allowing an earlier detection of ice than using a forward-looking housing configuration (Figure 12). The altimeter was connected to the science computer through the NOC hub by using a Subconn connector in the science bay instead of an integration in the nose cone, as a complete redesign of the nose would be required to accommodate a sensor of this size. Subconn connectors are widely used in Slocum gliders to connect turbulence and nutrient sensors with very good results. TWR already provides science bays with a single Subconn plug.

4 | Lab and Field Tests

An upward-looking altimeter, Impact Subsea ISA500, was integrated into a Slocum G2 glider, and the use of a backseat driver architecture to modify the glider's behavior based on sensor input was successfully trialed. These initial backseat driver trials were conducted off Mallorca at the Balearic Islands Coastal Observing and Forecasting facility where we used the glider temperature sensor to trigger a return to the surface when the water temperature dropped to a preprogrammed level. This work proved we could safely allow the glider to change behavior without user input, and solely on data from a sensor. During these early trials, we tested this behavior multiple times at different temperature settings, proving robust backseat driver capability during real-world operations. The aim of the tests in this section was to assess the performance of the upward-looking altimeter and the backseat driver in controlling gliders under ice.

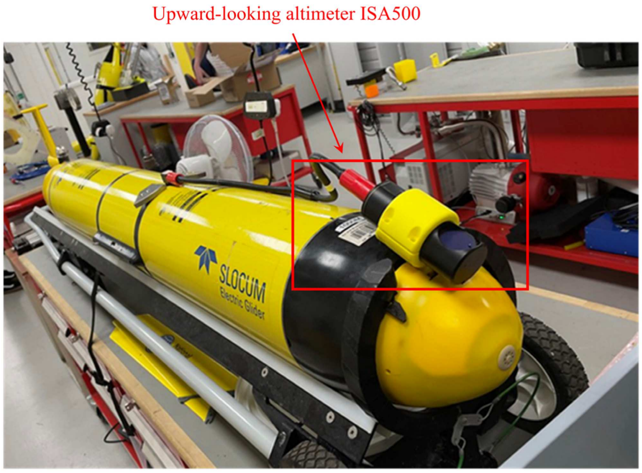

FIGURE 12 | A Slocum glider with an upward-looking altimeter ISA500 installed on top of it. [Color figure can be viewed at wileyonlinelibrary.com]

4.1 | Altimeter Glider Trials

An upward-looking altimeter is the key for under ice operations. However, the marginal ice zone poses significant challenges for upward-looking altimeters due to the presence of a mixture of seawater, freshwater, and ice which are prone to scattering altimeter acoustic pulses, leading to more variable performance compared with solid ice or open-water conditions. We conducted two trials to assess the altimeter's effectiveness in marginal ice zone conditions, which is an enabler for under-ice operations.

The first trial aimed to characterize the performance of the altimeter when deployed under-ice. Here, we carried out in-house tank tests to determine the performance of the altimeter specifically under marginal ice zone conditions. Marginal ice conditions occur at the edge of ice packs where the main body

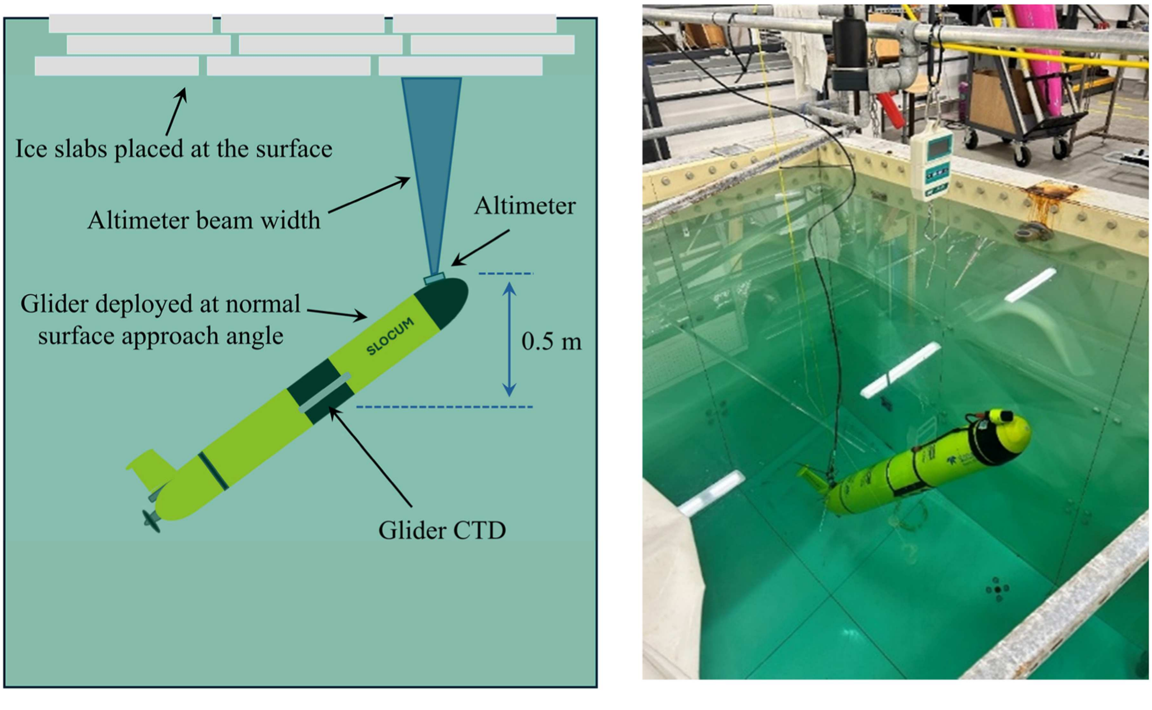

FIGURE 13 | Altimeter glider situated in National Oceanography Centre test tank: (a) illustration about the setup of the glider in the tank and (b) glider with a cable for command and control. CTD, conductivity–temperature–depth. [Color figure can be viewed at wileyonlinelibrary.com]

of ice ends and there is a mixture of broken melting ice and seawater. This is the region the glider is likely to attempt to surface after completing an under-ice operation and therefore important to be simulated during tank tests. The second trial was in the open-water area off Plymouth aiming to determine whether the upward-looking altimeter would detect the water surface during ascent.

4.1.1 | Altimeter Test in the Tank with Ice

A glider was placed in a 4-m deep seawater ballasting tank, positioned to match the normal surface approach angle (Figure 13a). A cable linked the glider to a command-and-control system next to the tank, facilitating full control and monitoring (Figure 13b). Throughout the experiment, the glider's depth within the tank was adjustable, enabling modifications to the altimeter range (upward-looking altitude) relative to the surface. Initially, the setup was used to evaluate the altimeter's performance in the absence of ice cover. Subsequently, ice slabs were placed on the tank's surface to assess the altimeter's performance in marginal ice zone conditions. The thickness of ice in the marginal ice zone varies from several centimeters to meters (Lange et al. 1989). Thicker ice is easier to detect by comparing depth from a pressure sensor and water column thickness from an upward altimeter, so accurate results on thin ice suggest a method capable of working on thicker ice. Accordingly, ice slabs with a thickness of 0.1 m were used in the tank experiment to establish how well the upward-looking altimeter can work in marginal ice zone conditions. Figure 13b illustrates the experimental configuration without ice cover.

TABLE 1 | Altimeter performance data in tank tests with no ice.

Glider depth (m)	Altimeter range (m)	Altimeter energy level	Altimeter correlation
2.45	1.95	0.527	0.98
2.27	1.77	0.52	0.97
1.96	1.46	0.59	0.97
1.63	1.14	0.50	0.95
1.23	0.75	0.32	0.92
0.96	10.2	0.18	0.54

In the ice-free test phase, the glider's depth was systematically lowered in six steps, ranging from 2.45 to 0.96 m. At each depth decrement, altimeter data such as range, energy levels, and correlation were collected (Table 1). The energy level received by the ISA500 receiver is measured from a metric between 0 and 1, with 1 indicating that the receiver is saturated with maximum energy. An energy level of 0.707 is the theoretical maximum (Impact Subsea 2024). The correlation factor, also on a scale of 0–1, signifies the quality of the returned echo. A value of 1 suggests minimal noise and distortion in the echo return. It could serve as a standalone trust indicator; lower values like 0.3 imply a higher likelihood of a false return. Combining this data with the energy level offers a more comprehensive assessment.

The altimeter readings showed a strong correlation with the glider depth measurements (Table 1). Glider depth is determined from the CTD, positioned 0.5 m below the altimeter's measuring face (Figure 13). Thus, a 0.5-m difference between glider depth and altimeter range indicates accurate altimeter readings. When the glider depth is 0.96 m, both altimeter correlation and energy levels are low, rendering the altimeter readings unreliable. Despite the manufacturer's asserted minimum range of 0.1 m, it is conceivable that acoustic reverberation conditions in the tank might be elevating this minimum range.

Figure 14 illustrates a simulation of the marginal ice cover in the NOC test tank. The glider, deployed beneath the ice with

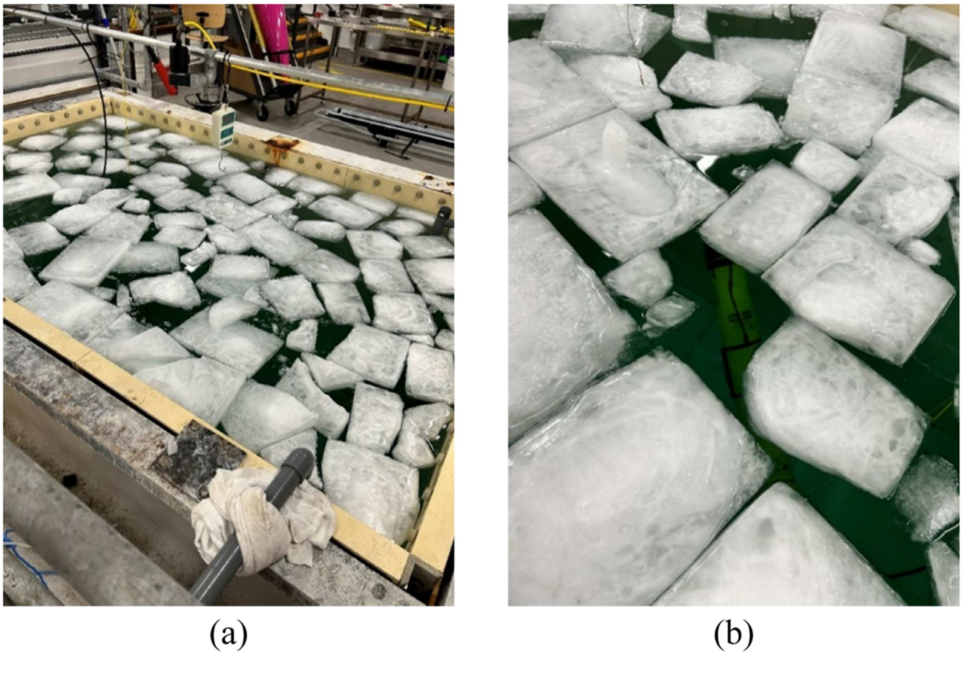

FIGURE 14 | Simulated marginal ice cover in the National Oceanography Centre test tank: (a) test tank with ice cover and (b) a glider being deployed below the ice cover. [Color figure can be viewed at wileyonlinelibrary.com]

a standard surface approach angle, experienced variations from 2.31 to 1.3 m glider depth, influencing the altimeter range to the ice-covered surface, as in previous deployments. In contrast to the earlier tank trial, the results under ice cover exhibit more variability in both range measurements and correlation values (Table 2). Throughout the experiment, the altimeter energy levels were notably lower compared with the tests without ice.

By examining the altimeter correlation in both no-ice and ice-covered experiments, it becomes evident that there is increased variability in the correlation measurement under ice conditions. This variability is likely linked to the marginal ice conditions simulated in the tank. Altimeter acoustic pulses will encounter seawater, freshwater and ice and bounce off ice block edges. These conditions will create variability and potentially contribute to the correlation measurements observed. The method of calculating the difference between the glider depth and the altimeter range proved ineffective for deriving ice draft and predicting the presence of ice in the marginal ice conditions created in the test tank with thin ice. Alternative approaches, such as analyzing the acoustic properties of water/ice and water/air scattered signals, may hold greater potential. Implementing these techniques would necessitate real-time analysis of the raw altimeter data onboard the glider. While feasible, this would likely require the development of highly efficient algorithms to produce usable results, which was considered too advanced for the scope of this initial study.

TABLE 2 | Altimeter performance data in tank tests with ice cover.

Glider depth (m)	Altimeter range (m)	Altimeter energy level	Altimeter correlation
2.31	1.92	0.24	0.89–0.77
1.95	1.46	0.13	0.81–0.51
1.63	1.18	0.13	0.93–0.53
1.30	0.91	0.13–0.55	0.96–0.91

4.1.2 | *Altimeter Test in Open Water*

A Slocum glider, unit 330, was deployed on January 23, 2023, within a survey approximately 20 nautical miles southwest of Plymouth. The site, with an average water depth of 65 m, provided an ideal environment for testing. To conserve power, the upward-looking altimeter was only activated during ascent, as the mission aimed to assess its performance in detecting the ocean surface. Altimeter altitude data were transmitted at each surfacing via the Iridium satellite network. Consistently, the altimeter began to detect the surface when the glider was approximately 25 m below it. Figure 15 illustrates the glider's depth from its CTD sensor alongside the altimeter range. As the glider neared the surface, the altimeter started to report the range to the surface. At other times, the altimeter reported a maximum range of 120 m, indicating it was beyond its detection range.

Figure 15 also shows a calculation of depth as recorded by the glider CTD sensor subtracted from the altimeter altitude. The glider has a large mass and reacts slowly to pressure changes caused by surface waves. The altimeter measures the instantaneous range to the surface. In theory, this calculation should measure the wave action at the surface. During this trial, no actual independent wave height measurement was taken; we observed that the measured average wave height was similar to the forecast average wave heights recorded throughout the mission.

4.2 | Backseat Driver Test in the Open Water

With an objective of integrating onboard sensors and backseat drive behaviors to enable an under-ice glider to attempt to detect and avoid unexpected ice conditions, two gliders (Gliders 305 and 330, see Figure 16) equipped with the backseat driver system were deployed from the RRS Discovery to the Greater Haig Fras site (around 50°18.711′ N, 7°29.690′ W) for open-water tests in June 2023. Following the successful completion of a shallow mission, which confirmed the gliders were in good condition, a series of missions was conducted. During this trial,

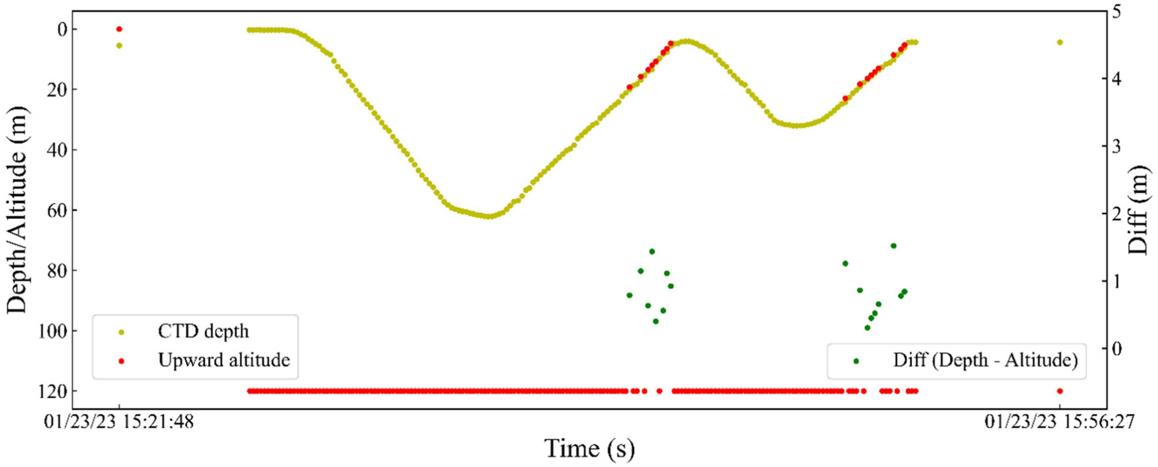

FIGURE 15 | An example of altimeter operation as the glider approaches the surface. CTD, conductivity–temperature–depth. [Color figure can be viewed at wileyonlinelibrary.com]

all the backseat driver features were successfully tested in water. The trial also provided pilots with valuable insights into adjusting the trim of the gliders to optimize backseat driver settings.

FIGURE 16 | Gliders 305 and 330 onboard RRS Discovery before open-water missions. [Color figure can be viewed at wileyonlinelibrary.com]

1. Heading control

   During a mission of approximately 50 h, which commenced around 10:00 on June 30, 2023, Glider 305 had its ice edge and ice draft strategies disabled, while all other ice-sensing strategies were engaged for ice detection. Midway through the mission, the glider's heading shifted from east to north (see Figure 17), aligning with the scheduled time for the desired heading change (08:30 on July 1, 2023), as defined in the backseat mission settings file. This demonstrates the ability of the backseat driver to adjust the glider's heading in real-time, allowing it to navigate out of ice areas, whether during a regular mission or in an emergency.

2. Depth and surfacing control

   In a separate mission conducted by Glider 305, where the ice draft ice-sensing strategy was activated, an unintended deep inflection occurred at a depth of 60 m when the upward-looking altimeter became operational (Figure 18). This inflection resulted from the backseat driver relying on outdated upward altitude data to control the depth before the altimeter was functioning

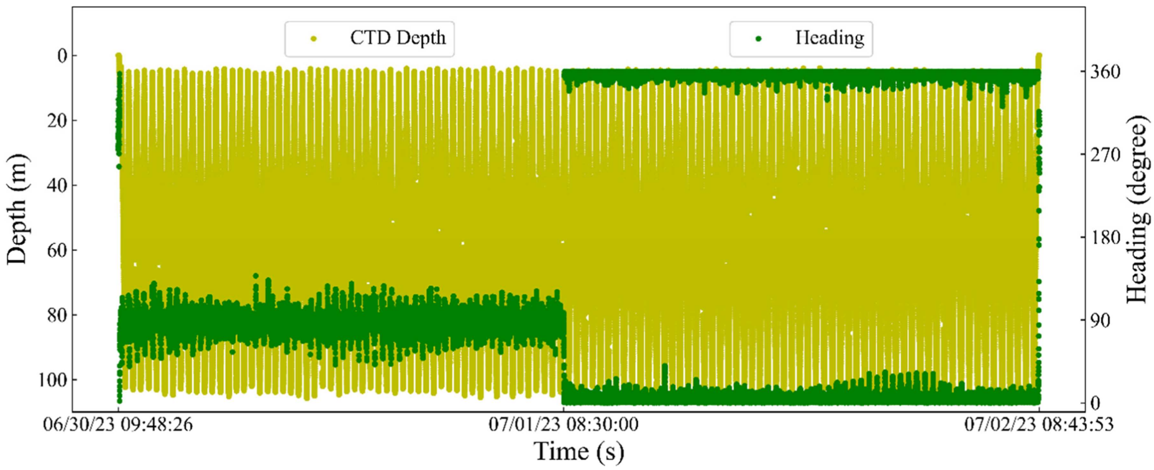

FIGURE 17 | A 50-h mission conducted by Glider 305 started on June 30, 2023, in which the backseat driver triggered a heading change at 08:30 on July 1, 2023. CTD, conductivity–temperature–depth. [Color figure can be viewed at wileyonlinelibrary.com]

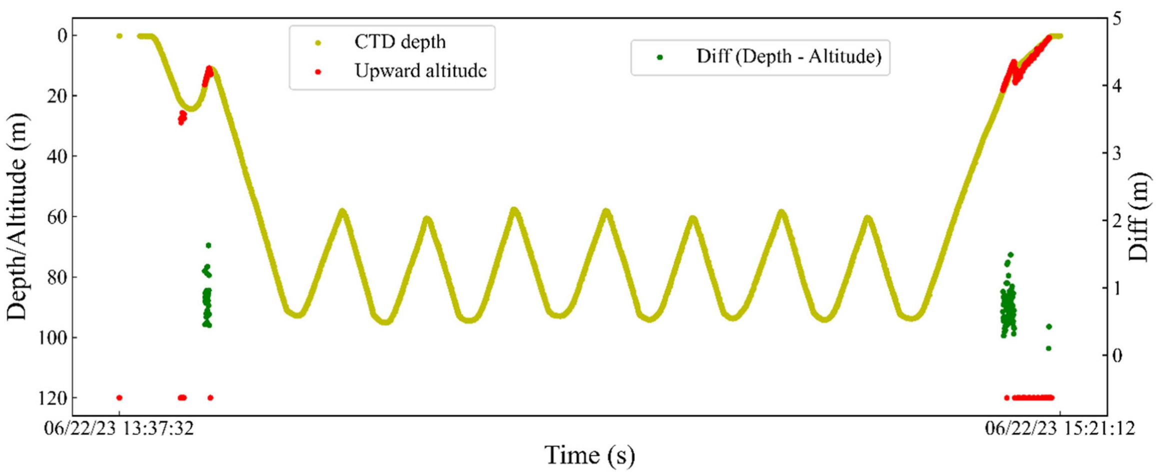

FIGURE 18 | A mission by Glider 305 with an undesired deep inflection at a depth of 60 m. CTD, conductivity–temperature–depth. [Color figure can be viewed at wileyonlinelibrary.com]

correctly, which was not presented in lab tests when the unintended setting on the backseat driver caused the data from the upward-looking altimeter to refresh before it could be processed. To prevent such inflections, introducing a delay in triggering the ice draft strategy until the upward altimeter is fully operational is an effective solution. Although in this mission the glider became trapped underwater because of the false upward-altitude data, it ultimately surfaced at the end. This was achieved by utilizing multiple urgency levels to control surfacing, which allowed the system to disregard the ice draft resulted from the inaccurate upward altitude when sensing the ice existence.

5 | Application—BIOPOLE Project in the Weddell Sea

Three Slocum gliders (Gliders 223, 438, and 444) were deployed in the Powell Basin of the northwestern Weddell Sea in early December 2023 (Figure 19), as part of a research cruise on *RRS Dir David Attenborough* undertaken by the National Capability Biogeochemical Processes and Ecosystem Function in Changing Polar Systems and Their Global Impacts (BIOPOLE) research program (Meijers et al. 2024). BIOPOLE is an interdisciplinary Natural Environment Research Council program examining biogeochemical processes and ecosystem function in polar ecosystems (https://biopole.ac.uk/). The inclusion of innovative autonomous underwater gliders allows for the collection of data over significantly extended durations and larger geographical areas than can be accomplished solely by ships. In addition to the glider missions, a range of physical, biological and biogeochemical observations were undertaken in the cruise, including CTD stations from which the glider instruments were calibrated, alongside ecological nets, nutrient and isotope analysis. The physical objectives of the cruise were to characterize the mixed layer during its springtime transition from a sea ice covered through a marginal ice zone and into the open water, and to examine the vertical transport of tracers between the deeper and shallower layers and the controls on that transport by submesoscale processes.

The gliders were deployed between 2500 and 4000 m of water close to the retreating, but variable, early summer sea ice edge. The aim was that the two vehicles (Gliders 223 and 438) equipped with backseat driver capability would transit approximately 20 km into and out of the sea ice to understand the differing physical and biological properties through the transition zone between open-water and sea-ice-covered conditions. While Antarctic sea ice extent in austral winter 2023 had been up to $2.5 \times 106\,km^2$ lower than usual, the local sea ice anomaly in the Powell Basin was relatively small. The ship-based sampling (along which the gliders were deployed) comprised a southeastward-oriented line from 62.5° S to 65.5° S (Meijers et al. 2024). This domain ranged from fully open, ice-free waters at the northern edge of Powell Basin, to broken ice up to 3/10 around the glider deployment site, to almost 10/10 coverage at the ice edge itself. While a fully comprehensive sea ice survey was not undertaken, ice conditions south of the edge varied between extremely thick multiyear ice at the northern end of the section (ridges of up to 5 m) with concentrations at or exceeding 8/10, to very large consolidated ice flows (up to 5 km) with significant leads further south (up to 7/10). During the period of the glider deployments, the ice generally retreated southward, though with much high-frequency variability dependent on passing storm systems, with the ice edge sometimes being heavily compacted and at other times with a relatively large marginal ice zone comprising ice floes of different sizes and open-water leads.

A total of 16 backseat driver missions were conducted, with 6 of these occurring beneath the sea ice (Table 3). All the missions ended with gliders following the instruction from the backseat driver to change its heading at the requested time, change its depth adaptively, and surface without

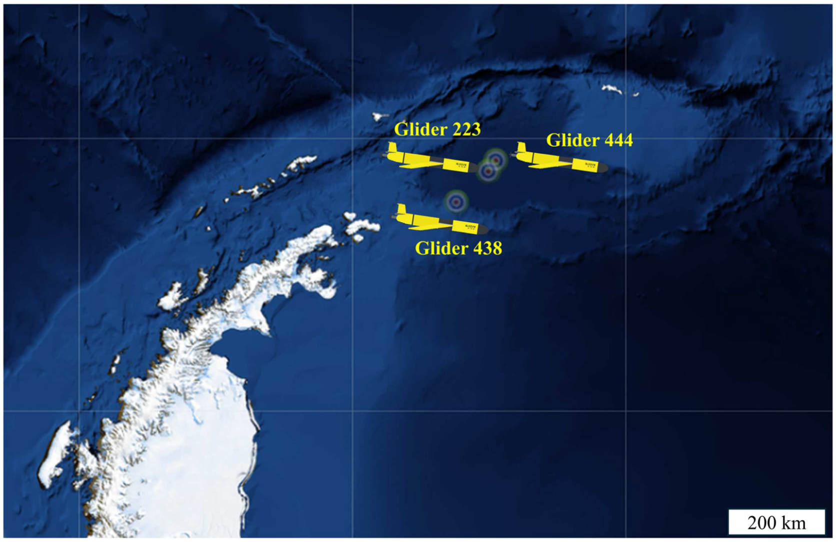

FIGURE 19 | Three Slocum gliders being deployed in the Weddell Sea for the BIOPOLE program. [Color figure can be viewed at wileyonlinelibrary.com]

TABLE 3 | Backseat driver (BSD) missions conducted by Gliders 223 and 438 in the BIOPOLE program.

No.	Mission start	Mission end	Mission type	Glider
1	December 6, 14:12:15, 2023	December 6, 16:36:32, 2023	BSD commissioning[a]	223
2	December 6, 17:43:59, 2023	December 7, 02:36:37, 2023	BSD commissioning[a]	223
3	December 8, 11:41:09, 2023	December 8, 13:58:44, 2023	BSD commissioning[a]	438
4	December 9, 07:31:24, 2023	December 9, 13:37:44, 2023	BSD commissioning[a]	438
5	December 9, 18:21:44, 2023	December 11, 21:01:10, 2023	Under ice	438
6	December 12, 13:01:26, 2023	December 13, 06:56:09, 2023	Ice approaching	438
7	December 13, 09:41:11, 2023	December 15, 11:09:33, 2023	Under ice	438
8	December 16, 14:19:47, 2023	December 17, 06:41:48, 2023	Ice approaching	438
9	December 17, 09:17:29, 2023	December 19, 17:35:02, 2023	Under ice	438
10	December 21, 19:20:01, 2023	December 23, 05:27:59, 2023	Under ice	223
11	December 27, 10:51:09, 2023	December 28, 10:32:17, 2023	Ice approaching	438
12	December 28, 11:29:58, 2023	December 30, 09:30:05, 2023	Under ice	438
13	January 9, 21:04:43, 2024	January 10, 11:22:45, 2024	Ice approaching	438
14	January 10, 12:48:24, 2024	January 11, 09:54:54, 2024	Ice approaching	438
15	January 11, 21:09:39, 2024	January 12, 09:17:20, 2024	Ice approaching	438
16	January 12, 10:05:40, 2024	January 14, 10:33:25, 2024	Under ice	438

[a]This is conducted in the open-water area.

colliding with ice. During the gliders' operation in this campaign, the update frequency of the remote-sensing products showing ice coverage varied from a few hours to 7 days, depending on the data source. However, the pilots typically received new ice coverage data at intervals of 1–2 days, a significant factor given the duration of the under-ice mission. Moreover, the glider relied on a simple dead-reckoning approach, which uses a compass and attitude sensor for navigation with unbounded navigation error. As a result, a predetermined surfacing location close to the ice edge may no longer be safe by the end of an under-ice mission. Consequently, the ice boundary strategy was not employed to control the glider's surfacing in any of the under-ice missions using backseat control. A minimum detectable submerged ice thickness of 5 m was used in all the under-ice missions when the ice draft strategy was used to control the surfacing. This threshold value was derived from the observation of ice from the ship and data collected in premission tests. Due to the setting in the configuration file to reduce the log file size and to save the communication time, the logged data being sent back remotely showed only a portion of the dead-reckoned path of the gliders.

TABLE 4 | Details of an under-ice mission conducted by Glider 438 from December 17 to December 19.

Item	Information
Mission start	December 17, 09:17:29, 2023
Expected surfacing time	December 19, 09:00:00, 2023
Surfacing time 1	December 19, 18:05:00, 2023
Surfacing time 2	December 19, 15:05:00, 2023
Surfacing time 3	December 19, 12:05:00, 2023
Heading 1	148.4°
Heading 2	326.6°
Heading change time	December 18, 09:00:00, 2023
Ice-sensing strategies	Median temperature of the upper water column, ice draft, Global Positioning System
Surfacing control	Ice-sensing strategies, mission time

1. Surfacing control

   During an over 2-day under-ice mission from December 17 to 19, 2023, Glider 438 was directed to head southeast (approximately 148° to the north) to enter the sea ice-covered area and then reverse its heading at 09:00 on December 18, 2023, to exit the sea-ice zone (Table 4 and Figure 20). The glider attempted to climb to the surface twice at 09:45 and 13:38 on December 19, 2023, to acquire GPS signals due to the low urgency level being reached: (1) the median temperature of the upper water column (from the depth of 20 to 50 m) exceeded the threshold temperature −1.78°C, indicating the absence of ice on the surface; (2) the measured ice draft was below the minimum detectable value of 5 m for the altimeter; (3) the mission time had surpassed the expected surfacing time. After waiting 20 min without receiving a GPS signal, the glider dived back to perform the yo behavior. The glider eventually climbed to the surface as the three urgency levels (low, median low, and median urgency level) indicated no ice on the surface, and successfully acquired a GPS fix at around 17:30. The surface behavior was then activated by the backseat driver and the mission was completed successfully.

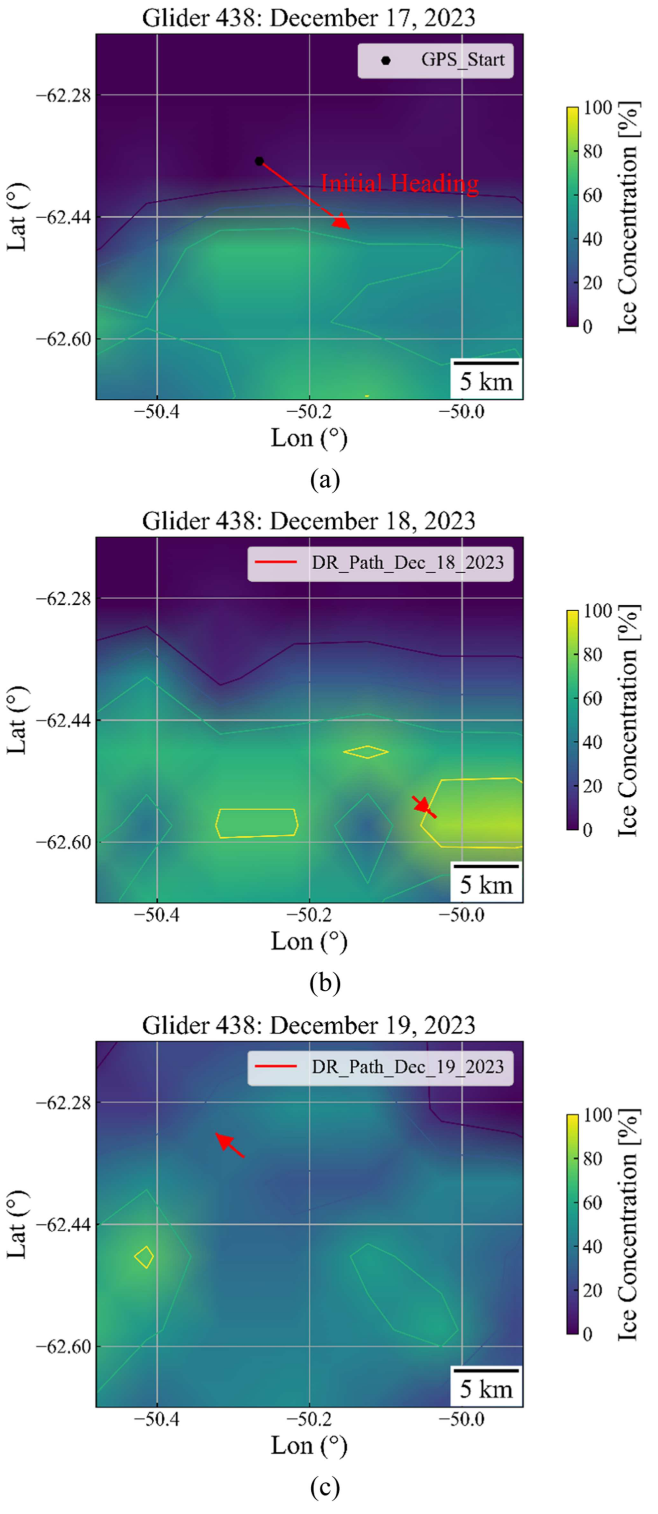

FIGURE 20 | An under-ice mission conducted by Glider 438 from December 17 to 19, 2023: (a) the GPS location of the glider at the mission start point and the initial heading of the glider, (b) a portion of the dead-reckoned (DR) path on December 18, 2023, and (c) a portion of the DR path on December 19, 2023. The ice concentration is from AMSR2 data (https://seaice.uni-bremen.de/data-archive/). AMSR, Advanced Microwave Scanning Radiometer; GPS, Global Positioning System. [Color figure can be viewed at wileyonlinelibrary.com]

TABLE 5 | Details of an under-ice mission conducted by Glider 223 from December 21 to December 23.

Item	Information
Mission start	December 21, 19:20:01, 2023
Mission end	December 23, 05:27:59, 2023
Heading 1	239.0°
Heading 2	290.0°
Heading change time	December 22, 11:00:00, 2023
Ice-sensing strategies	Median temperature of the upper water column, ice draft, Global Positioning System
Surfacing control	Ice-sensing strategies, mission time

2. Heading control

In the under-ice mission conducted by Glider 223 from December 21 to 23, the aim was to navigate through a tongue-shaped ice formation rather than to conduct an in-out reverse under-ice mission. The glider was commanded to follow a V-shape path, starting with an initial heading of 239° to the north, and then changing to 290° to the north to return from the opposite side of the ice tongue (Table 5). As a result of the previously mentioned configuration file setting, a portion of the dead-reckoned path was logged (Figure 21). The glider maintained the intended course based on visible data, and the measured heading after 11:00 on December 22, 2024 was shown as required. The mission was completed successfully with the glider surfacing in an open-water area free of ice cover.

3. Depth control

During a nearly 2-day mission conducted by Glider 438 from December 28 to 30, 2023, the dead-reckoned location of the glider was logged every 60 s in the log file. This logging enabled the extraction and visualization of nearly the entire dead-reckoned path of the glider from the mission (Figure 22). The glider collected data within a full depth range from close to the water surface to 1000 m (Figure 23), with its depth being controlled by the backseat driver after the first 20-m dive. The desired climb depth was 9 m, however, the glider climbed to around 14 m on its 5th yo and then dived. This occurred because the upward-looking altimeter detected ice, prompting the backseat driver to initiate a dive before reaching the initially intended climb depth. The glider was commanded to approach the surface slowly to get GPS signals at around 09:30 on December 30, successfully acquiring GPS signals without any further dives. By the end of the approximately 46-h mission, the dead-reckoned position had diverged from the GPS fix by around 8 km, highlighting the critical importance of accurate underwater navigation for gliders undertaking extended operations beneath ice.

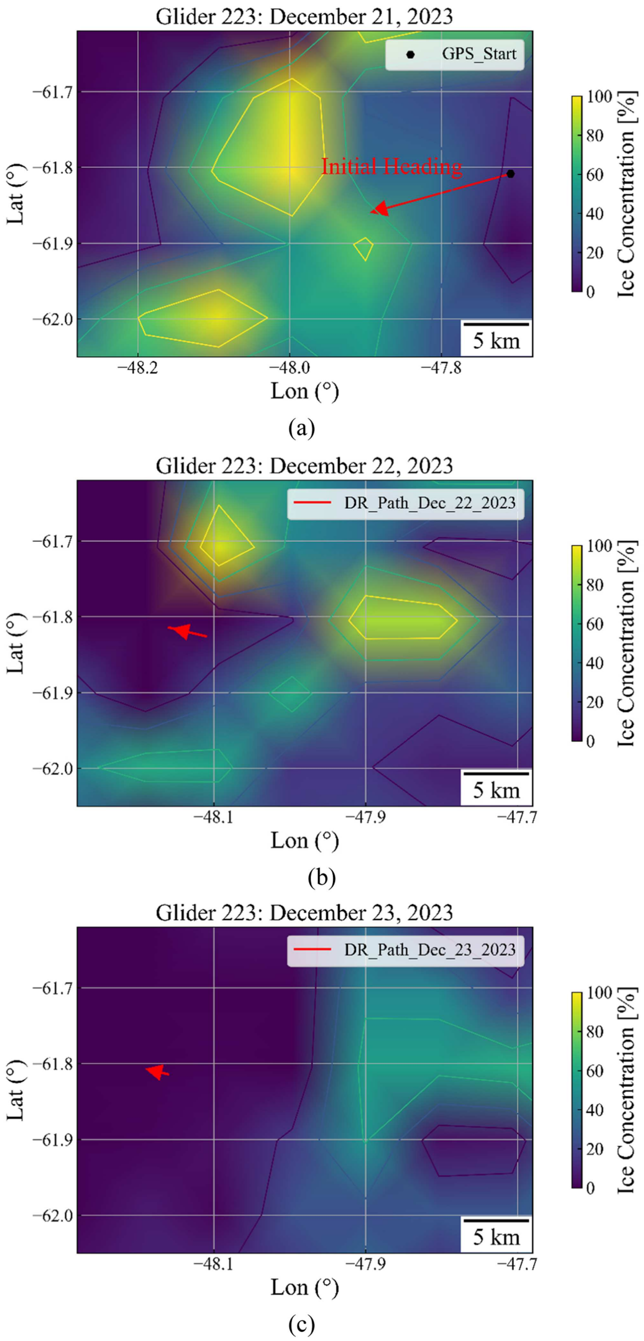

FIGURE 21 | An under-ice mission conducted by Glider 223 from December 21 to 23, 2023: (a) the GPS location of the glider at the mission start point and the initial heading of the glider, (b) a portion of the dead-reckoned (DR) path on December 22, 2023, and (c) a portion of the DR path on December 23, 2023. The ice concentration is from AMSR2 data (https://seaice.uni-bremen.de/data-archive/). AMSR, Advanced Microwave Scanning Radiometer; GPS, Global Positioning System. [Color figure can be viewed at wileyonlinelibrary.com]

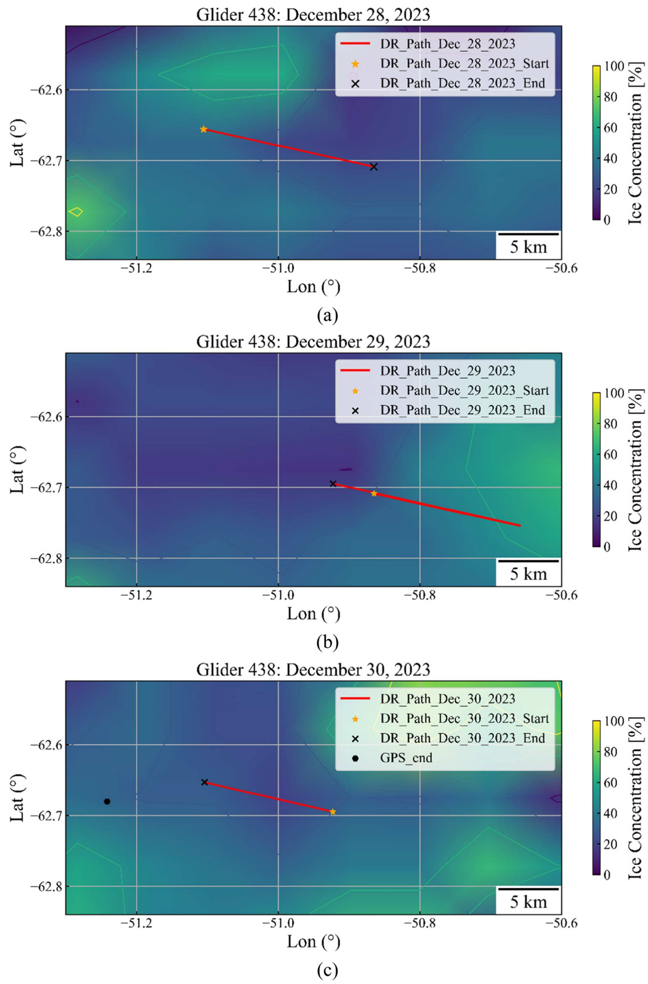

FIGURE 22 | An under-ice mission conducted by Glider 438 from December 28 to 30, 2023: (a) the dead-reckoned (DR) path on December 28, 2023, (b) the DR path on December 29, 2023, and (c) the DR path and GPS location on December 30, 2023. The ice concentration is from AMSR2 data (https://seaice.uni-bremen.de/data-archive/). AMSR, Advanced Microwave Scanning Radiometer; GPS, Global Positioning System. [Color figure can be viewed at wileyonlinelibrary.com]

4. Energy consumption

To evaluate the impact of the backseat driver system on energy efficiency, the energy consumption rate in scenarios with and without the system is compared. In both scenarios, the glider performed a mission with one yo with a diving depth of 1000 m. The battery usage was monitored in real-time using a coulomb counter, which measures the total charge consumed in ampere-hours. The energy consumption rate is represented by the average current draw, measured in amperes (Table 6). In the scenarios with the backseat driver system, the backseat driver computer remained powered on throughout the entire mission, while the upward-looking altimeter was activated only when the glider operated at depths shallower than 75 m.

The energy consumption rate increases with the use of the backseat driver system, with the backseat driver computer contributing significantly to power usage than the upward-looking altimeter. Since the backseat driver system is primarily used for ice detection when the glider is near the surface during short-term under-ice missions, the power consumption could be significantly reduced by activating the backseat driver computer only when necessary.

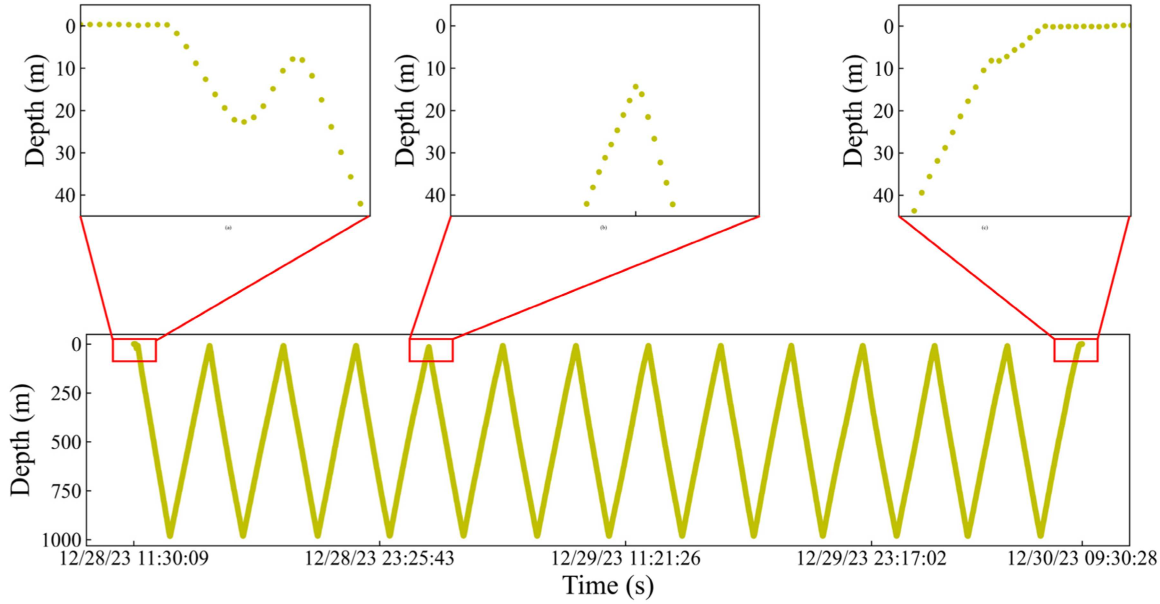

FIGURE 23 | The yo profiles in an under-ice mission conducted by Glider 438 from December 28 to 30, 2023. [Color figure can be viewed at wileyonlinelibrary.com]

TABLE 6 | Energy consumption rate for scenarios without and with backseat driver.

Scenario	Without backseat driver (A)	With backseat driver (A)
Diving with upward-looking altimeter		0.237–0.272
Diving or climbing without upward-looking altimeter	0.081–0.093	0.236–0.247
Diving then climbing without upward-looking altimeter	0.150–0.156	0.322–0.410

6 | Conclusions and Future Work

This work presents a high-level architecture that integrates a backseat driver system with an upward-looking altimeter for Slocum gliders to enable short-term missions under sea ice. The backseat driver monitors data from various gilder sensors (e.g., depth, temperature, and upward-looking altitude) and autonomously responds to this information without direct user intervention. The upward-looking altimeter measures the distance to the ice above and the ice draft, aiding in ice avoidance and ensuring safe surfacing. However, trials with the altimeter revealed its limitations in detecting thin ice. Consequently, the altimeter alone is not sufficient for under-ice missions controlled by a backseat driver system. To address this, multiple ice-sensing strategies were employed, including monitoring the median temperature of the upper water column, detecting the ice edge, and acquiring GPS signals in addition to monitoring ice draft. These ice-sensing strategies, combined with mission time, are used to manage surfacing in various urgent situations, ensuring that the glider can surface even if one ice-sensing strategy fails.

The localization error generated by dead reckoning was not addressed in this work due to the fact that uncertainty in underwater localization can generally be ignored in short-term under ice missions. Additionally, the uncertainty in ice-sensing strategy caused by using ice edge with poor positioning can be managed by urgency levels. However, for long-term under ice missions where gliders must profile a specific area, accurate underwater localization becomes crucial. Enhancing the Slocum glider's underwater localization capabilities will improve its safe operation beneath the ice and ensure data collection in the target area. Future efforts will focus on refining and advancing long-term ice-handling functionalities.

Acknowledgments

This work was supported by the BIOPOLE National Capability Multicentre Round 2 funding from the Natural Environment Research Council (Grant No. NE/W004933/1) and by the European Union's Horizon 2020 research and innovation program under Grant No. 821001 (SO_CHIC).

Data Availability Statement

The data that support the findings of this study are available from the corresponding author upon reasonable request.

References

Andersson, T. R., J. S. Hosking, M. Pérez-Ortiz, et al. 2021. “Seasonal Arctic Sea Ice Forecasting With Probabilistic Deep Learning.” *Nature Communications* 12, no. 1: 5124. https://doi.org/10.1038/s41467-021-25257-4.

Brierley, A. S. 2001. *RRS James Clark Ross Cruise 58 Autosub Cruise*.

Brierley, A. S., P. G. Fernandes, M. A. Brandon, et al. 2002. “Antarctic Krill Under Sea Ice: Elevated Abundance in a Narrow Band Just South of Ice Edge.” *Science* 295, no. 5561: 1890–1892. https://doi.org/10.1126/science.1068574.

Chassignet, E. P., S. G. Yeager, B. Fox-Kemper, et al. 2020. "Impact of Horizontal Resolution on Global Ocean-Sea Ice Model Simulations Based on the Experimental Protocols of the Ocean Model Intercomparison Project Phase 2 (OMIP-2)." *Geoscientific Model Development* 13, no. 9: 4595–4637. https://doi.org/10.5194/GMD-13-4595-2020.

Cochlan, W. 2008. "Nitrogen Uptake in the Southern Ocean." In *Nitrogen in the Marine Environment*, edited by D. G. Capone, D. A. Bronk, M. R. Mulholland, and E. J. Carpenter, 569–596. Academic Press, Elsevier.

Coppolaro, V. 2018. *Sea Ice Underside Three-Dimensional Topography and Draft Measurements With an Upward-Looking Multibeam Sonar Mounted on a Remotely Operated Vehicle Relatore: Candidato*. Università di Firenze.

Eickstedt, D. P., and S. R. Sideleau. 2009. "The Backseat Control Architecture for Autonomous Robotic Vehicles: A Case Study With the Iver2 AUV." In *OCEANS 2009*, 1–8. https://doi.org/10.23919/OCEANS.2009.5422212.

Engdahl, J., J. Gradone, Z. Silva, D. Aragon, N. Shivakumar, and T. Miles. 2023. "Implementation of Near Real-Time Onboard Processing Software for a Slocum Glider Acoustic Doppler Current Profiler." In *OCEANS 2023—MTS/IEEE U.S. Gulf Coast*, 1–5. https://doi.org/10.23919/OCEANS52994.2023.10337179.

Fanelli, F., D. Fenucci, R. Marlow, A. Morris, R. Templeton, and A. Phillips. 2025. "Deploying Autosub Long Range Under the Dotson Ice Shelf: An Engineering Perspective." In *OCEANS 2025 Brest*, 1–10. https://doi.org/10.1109/OCEANS58557.2025.11104354.

Ferguson, J. S. 1998. "The Theseus Autonomous Underwater Vehicle Two Successful Missions." In *UT 1998—Proceedings of the 1998 International Symposium on Underwater Technology*, 109–114. https://doi.org/10.1109/UT.1998.670072.

Gallimore, E., R. Stokey, and E. Terrill. 2018. "Robot Operating System (ROS) on the REMUS AUV Using RECON." In *2018 IEEE/OES Autonomous Underwater Vehicle Workshop (AU)*, 1–6. https://doi.org/10.1109/AUV.2018.8729755.

Impact Subsea. 2024. *ISA500 Underwater Altimeter & Echosounder Installation & Operation Manual*.

Jones, C., B. Allsup, and C. DeCollibus. 2014. "Slocum Glider: Expanding Our Understanding of the Oceans." In *2014 Oceans—St. John's*, 1–10. https://doi.org/10.1109/OCEANS.2014.7003260.

Kaminski, C., T. Crees, J. Ferguson, et al. 2010. "12 Days Under Ice—An Historic AUV Deployment in the Canadian High Arctic." In *2010 IEEE/OES Autonomous Underwater Vehicles*, 1–11. https://doi.org/10.1109/AUV.2010.5779651.

Keane, J. R., A. L. Forrest, H. Johannsson, and D. Battle. 2020. "Autonomous Underwater Vehicle Homing With a Single Range-Only Beacon." *IEEE Journal of Oceanic Engineering* 45, no. 2: 395–403. https://doi.org/10.1109/JOE.2018.2877535.

Kerlin, K. 2019. *Robotic Glider Makes First Turbulence Measurements Beneath an Antarctic Ice Shelf*. University of California, Davis. https://phys.org/news/2019-02-robotic-glider-turbulence-beneath-antarctic.html.

Klatt, O., O. Boebel, and E. Fahrbach. 2007. "A Profiling Float's Sense of Ice." *Journal of Atmospheric and Oceanic Technology* 24, no. 7: 1301–1308. https://doi.org/10.1175/JTECH2026.1.

Lange, M. A., S. F. Ackley, P. Wadhams, G. S. Dieckmann, and H. Eicken. 1989. "Development of Sea Ice in the Weddell Sea." *Annals of Glaciology* 12: 92–96. https://doi.org/10.3189/S0260305500007023.

McPhail, S., R. Templeton, M. Pebody, D. Roper, and R. Morrison. 2019. "Autosub Long Range AUV Missions Under the Filchner and Ronne Ice Shelves in the Weddell Sea, Antarctica—An Engineering Perspective." In *OCEANS 2019—Marseille*, 1–8. https://doi.org/10.1109/OCEANSE.2019.8867206.

Meijers, A., N. Johnston, L. Taylor, G. Stowasser, A. Brearley, and P. ten Hoopen. 2024. *Cruise Report for Voyage SD033 of the RRS Sir David Attenborough—BIOPOLE I*. British Antarctic Survey. https://www.bodc.ac.uk/resources/inventories/cruise_inventory/reports/sd033.pdf.

Montie, S., M. S. Thomsen, W. Rack, and P. A. Broady. 2020. "Extreme Summer Marine Heatwaves Increase Chlorophyll a in the Southern Ocean." *Antarctic Science* 32, no. 6: 508–509. https://doi.org/10.1017/S0954102020000401.

Murphy, S. R. 1972. *Arctic Technology Development at the University of Washington*, 1–88.

Naglak, J. E., B. R. Page, and N. Mahmoudian. 2018. "Backseat Control of SandShark AUV Using ROS on RaspberryPi." In *OCEANS 2018 MTS/IEEE Charleston*, 1–5. https://doi.org/10.1109/OCEANS.2018.8604630.

Rintoul, S. R. 2018. "The Global Influence of Localized Dynamics in the Southern Ocean." *Nature* 558, no. 7709: 209–218. https://doi.org/10.1038/s41586-018-0182-3.

Riser, S. C., D. Swift, and R. Drucker. 2018. "Profiling Floats in SOCCOM: Technical Capabilities for Studying the Southern Ocean." *Journal of Geophysical Research: Oceans* 123, no. 6: 4055–4073. https://doi.org/10.1002/2017JC013419.

Sallée, J. B., V. Pellichero, C. Akhoudas, et al. 2021. "Summertime Increases in Upper Ocean Stratification and Mixed Layer Depth." *Nature* 591, no. 7851: 592–598. https://doi.org/10.1038/S41586-021-03303-X.

Sugimoto, S. 2022. "Decreasing Wintertime Mixed-Layer Depth in the Northwestern North Pacific Subtropical Gyre." *Geophysical Research Letters* 49, no. 2: e2021GL095091. https://doi.org/10.1029/2021GL095091.

Wang, Y., N. Bose, W. Thanyamanta, C. Bulger, and S. Shaikh-Upadhye. 2022. "Adaptive Control for Follower Gliders Mapping Underwater Oil Patches." *Journal of Hazardous Materials* 436: 129039. https://doi.org/10.1016/j.jhazmat.2022.129039.

Wang, Y., C. Bulger, W. Thanyamanta, and N. Bose. 2021. "A Backseat Control Architecture for a Slocum Glider." *Journal of Marine Science and Engineering* 9, no. 5: 532. https://doi.org/10.3390/jmse9050532.

Wang, Y., G. Salavasidis, B. Allsup, et al. 2025. "Enhancing Slocum Gliders for Extended Polar Science." In *OCEANS 2025 Brest*, 1–6. https://doi.org/10.1109/OCEANS58557.2025.11104646.

Webster, S. E., C. M. Lee, and J. I. Gobat. 2014. "Preliminary Results in Under-Ice Acoustic Navigation for Seagliders in Davis Strait." In *IEEE/MTS Oceans Conference and Exhibition*, 1–5. https://doi.org/10.1109/OCEANS.2014.7003070.

Woithe, H. C., D. Boehm, and U. Kremer. 2011. "Improving Slocum Glider Dead Reckoning Using a Doppler Velocity Log." In *OCEANS'11 MTS/IEEE KONA*, 1–5. https://doi.org/10.23919/OCEANS.2011.6107296.